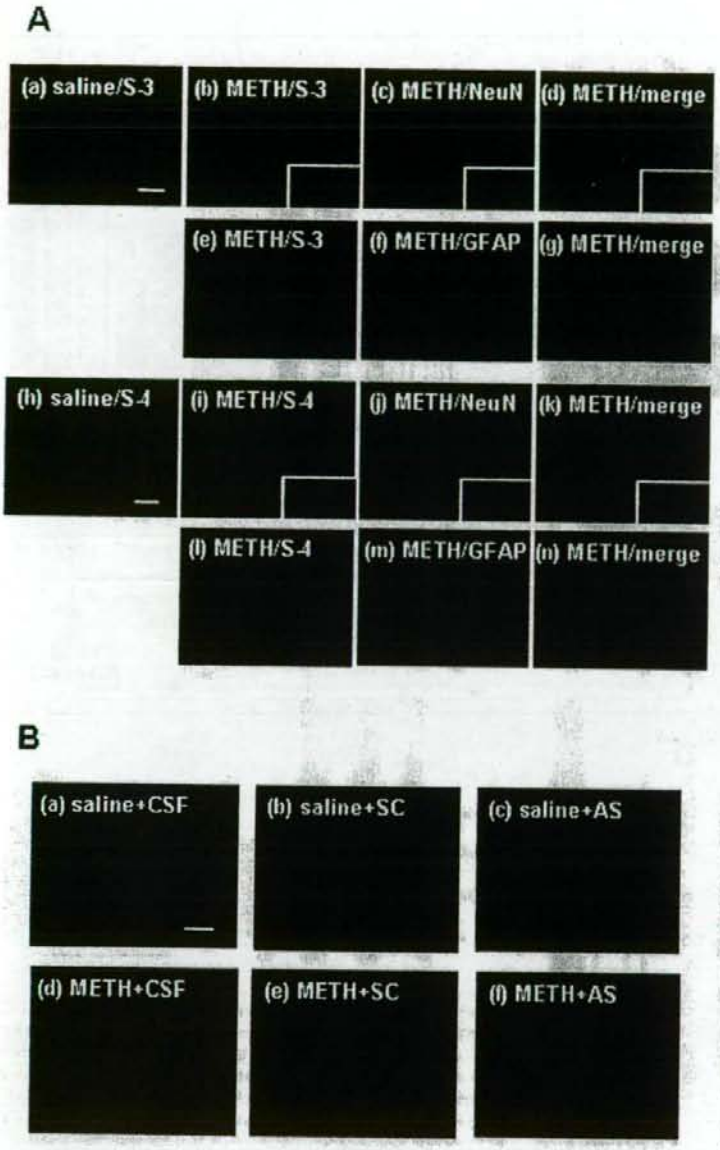

Figure 4. Immunostaining of shati in the NAc after repeated treatment with METH. Mice were administered METH (2 mg/kg, s.c.) for 6 d and decapitated 24 h after the last treatment. ***A***, Double-labeling fluorescence photomicrographs for shati and NeuN or GFAP. The shati-immunopositive cells (green) were colocalized with NeuN-immonopositive cells (red). Double immunostaining for S-3 or S-4 and NeuN in the NAc reveals shati expression in neuronal cells. Scale bars, 20 μm. ***B***, Effect of shati-AS on METH-induced increase in shati expression. METH-induced increase in shati expression in the NAc was inhibited by shati-AS. Scale bar, 20 μm.

D_1-like receptor antagonist $R(+)$-SCH23390 (0.1 mg/kg, i.p.) or the D_2-like receptor antagonist raclopride (2 mg/kg, i.p.) (agonist, $F_{(1,34)} = 18.649$, $p < 0.01$; antagonist, $F_{(2,34)} = 5.554$, $p < 0.01$; agonist × antagonist, $F_{(2,34)} = 5.382$, $p < 0.01$; two-way ANOVA) (Fig. 3*D*), although neither antagonists had an effect on shati mRNA expression in the saline-treated mice. These results indicate that METH induces the expression of shati mRNA in the brain through the activation of both DA D_1 and D_2 receptors.

Localization of shati in the brain of mice treated with METH

There were few shati-immunopositive cells in saline-treated mouse brain (Fig. 4*Aa*,*Ah*). METH (2 mg/kg, s.c. for 6 d) increased the number of shati-immunopositive cells in the NAc compared with that in saline-treated mice (Fig. 4*A*). The shati-immunopositive cells were diminished when the antibodies were absorbed by S-3 or S-4 antigen (data not shown). The shati-immunopositive cells were colocalized with the cells that were immunopositive for NeuN, a neuronal marker, but not for GFAP, an astroglial marker, in the NAc of mice (Fig. 4*Ab–Ag*,*Ai–An*). The repeated METH treatment-induced increase in the numbers of shati-immunopositive cells in the NAc was abolished by shati-AS treatment, although shati-SC had no effect (Fig. 4*Ba–Bf*).

Roles of shati in METH-induced hyperlocomotion and sensitization

To examine the role of shati in the behavioral and neurochemical phenotype in response to METH, we used an AS strategy, which widely used to manipulate gene expression in the brain via intracerebroventricular infusion (Taubenfeld et al., 2001; Bowers et al., 2004). The experimental schedules are shown in Figure 5, *A* and *C*. The AS downregulated the expression of shati mRNA in the NAc (Fig. 5*B*). The increase in the levels of shati mRNA expression evoked by repeated METH treatment in the NAc was significantly and completely abolished by shati-AS, although shati-SC had no effect. Moreover, shati mRNA expression in the NAc of saline-treated mice was also reduced by shati-AS, whereas shati-SC did not affect the expression in saline-treated mice (drug, $F_{(1,42)} = 72.765$, $p < 0.01$; intracerebroventricular treatment, $F_{(2,42)} = 14.104$, $p < 0.01$; drug × intracerebroventricular treatment, $F_{(2,42)} = 0.092$, $p = 0.912$; two-way ANOVA) (Fig. 5*B*), indicating that shati-AS has an ability to reduce effectively the expression of shati mRNA. We also examined the effect of shati-AS on tPA expression as one of drug-dependence-related other proteins, because tPA–plasmin system potentiates the rewarding and locomotor-stimulating effects of METH, MOR, and nicotine by regulating release of DA (Nagai et al., 2004, 2005a,b, 2006). The increase in the levels of tPA mRNA expression in the NAc was not abolished by shati-AS (drug, $F_{(1,47)} = 62.530$, $p < 0.01$; intracerebroventricular treatment, $F_{(2,47)} = 0.148$, $p = 0.862$; drug × intracerebroventricular treatment, $F_{(2,47)} = 0.803$, $p = 0.454$; two-way ANOVA). Moreover, tPA mRNA expression in the NAc of saline-treated mice was not also reduced by shati-AS, indicating that shati-AS has no ability to

reduce effectively the expression of tPA mRNA (data not shown). Therefore, shati-AS is considered to have no secondary effects.

Repeated METH administration leads to a progressive augmentation of many behavioral effects of the drug (behavioral sensitization). Sensitization is of interest as a model for drug-induced neuroplasticity in neuronal circuits important for addiction. It is well established that the induction of sensitization involves complex neuronal circuitry (Wolf, 1998). In rodent, sensitization is observed as a progressive augmentation of locomotor activity that may relate to an increase in the incentive to obtain drugs (Robinson and Berridge, 1993; Lorrain et al., 2000). There is also evidence of sensitization in human drug users (Satel et al., 1991) and normal subjects (Strakowski and Sax, 1998). Repeated METH treatment (1 and 2 mg/kg, s.c.) for 5 d produced behavioral sensitization [$F_{(2,12)} = 7.404$ for METH (1 mg/kg) plus shati-AS-treated mice; $F_{(2,18)} = 5.593$ for METH (1 mg/kg) plus shati-SC-treated mice; $F_{(2,18)} = 30.917$ for METH (1 mg/kg) plus CSF-treated mice; $F_{(2,12)} = 7.453$ for METH (2 mg/kg) plus shati-AS-treated mice, $F_{(2,12)} = 4.243$ for METH (2 mg/kg) plus shati-SC-treated mice; $F_{(2,15)} = 8.569$ for METH (2 mg/kg) plus CSF-treated mice; $p < 0.05$, one-way ANOVA] (Fig. 5*D*). As shown in Figure 5*D*, the shati-AS treatment potentiated the METH (1 mg/kg, s.c.)-induced hyperlocomotion and sensitization compared with shati-SC- or CSF-treated mice (drug, $F_{(2,141)} = 291.696$, $p < 0.01$; intracerebroventricular treatment, $F_{(2,141)} = 28.223$, $p < 0.01$; time, $F_{(2,141)} = 17.154$, $p < 0.01$; drug × intracerebroventricular treatment, $F_{(4,141)} = 12.432$, $p < 0.01$; drug × time, $F_{(4,141)} = 12.913$, $p < 0.01$; intracerebroventricular treatment × time, $F_{(4,141)} = 0.156$, $p = 0.960$; drug × intracerebroventricular treatment × time, $F_{(8,141)} = 0.427$, $p = 0.903$; three-factor repeated ANOVA), whereas the shati-AS, shati-SC, or CSF treatment had no effect on spontaneous locomotor activity (Fig. 5*D*). The sensitization was observed on day 10 after challenge administration of METH (0.3 mg/kg, s.c.). Shati-AS-treated mice showed a marked potentiation of METH (0.3 mg/kg, s.c.)-induced sensitization on day 10 compared with shati-SC- or CSF-treated mice ($F_{(2,13)} = 6.974$, $p < 0.05$, one-way ANOVA), although shati-AS-treated mice did not show a potentiation of METH (2 mg/kg, s.c.)-induced hyperlocomotion and sensitization compared with shati-SC- or CSF-treated mice on days 1–5 (Fig. 5*D*).

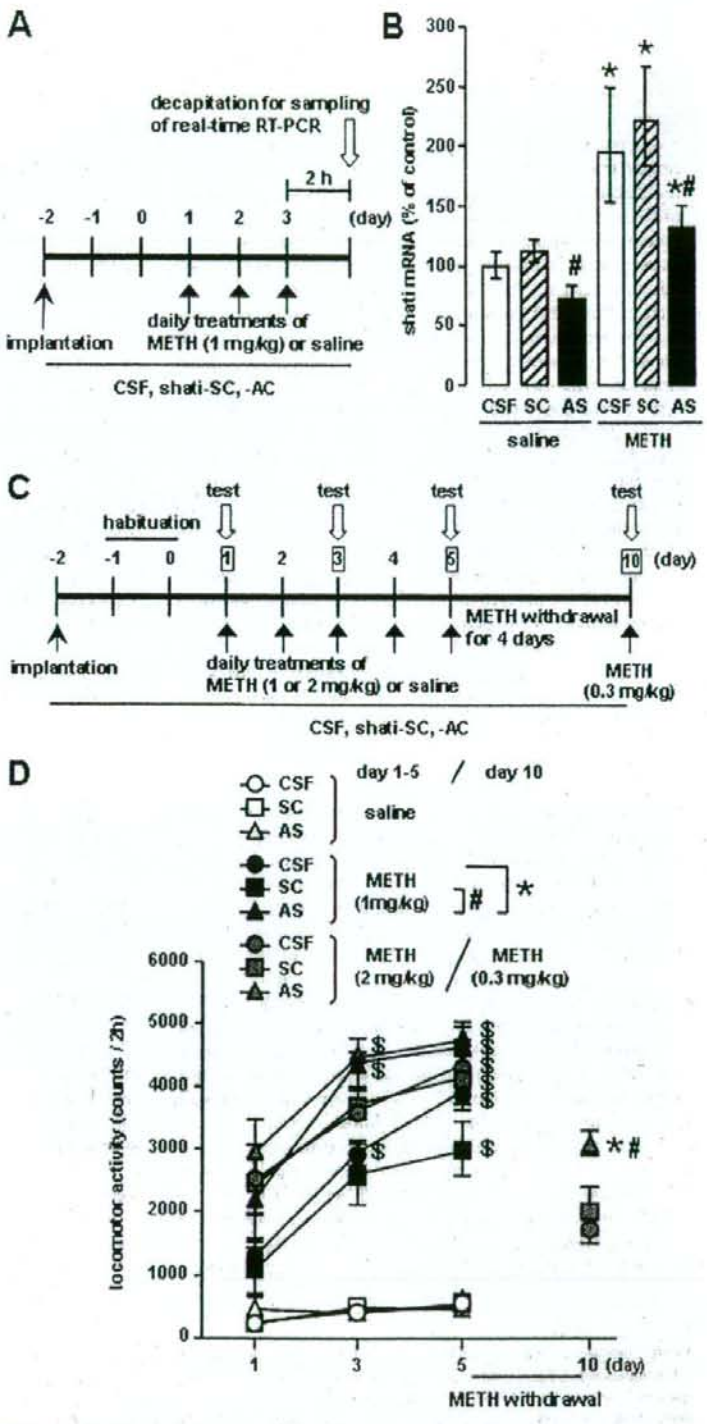

Figure 5. Roles of shati in METH-induced hyperlocomotion and sensitization. An osmotic minipump was used to deliver a continuous infusion of shati-AS (1.8 nmol/6 μl per day), shati-SC (1.8 nmol/6 μl per day), or CSF into the right ventricle (AP −0.5 mm, ML +1.0 mm from bregma, and DV −2.0 mm from the skull). ***A***, Experimental schedule for the real-time RT-PCR using shati-AS. ***B***, Effect of shati-AS on shati mRNA expression. Mice were administered METH (1 mg/kg, s.c.) for 3 d and decapitated 2 h

Roles of shati in METH-induced dopaminergic responses

The pharmacological effects of METH are linked to its capacity to elevate extracellular DA levels by releasing DA from presynaptic nerve terminals and inhibiting its reuptake (Heikkila et al., 1975; Seiden et al., 1993). In addition, METH and the amphetamines redistribute DA from synaptic vesicles to the cytosol and promote reverse transport (Seiden et al., 1993). Therefore, we examined the effect of shati-AS on the METH-induced increase in overflow of DA in the NAc using an *in vivo* microdialysis technique. The experimental schedule is shown in Figure 6*A*. METH caused a marked increase in overflow of DA in the NAc of the CSF-treated mice on the day 3 (Fig. 6*B*). The peak of overflow of DA was increased by METH treatment to ~360% of the baseline level in the CSF-treated mice. In shati-AS-treated mice, the METH-induced increase in overflow of DA was significantly potentiated compared with that in the shati-SC- or CSF-treated mice (intracerebroventricular treatment, $F_{(2,14)} = 5.662$, $p < 0.05$; time, $F_{(10,140)} = 35.646$, $p < 0.01$; intracerebroventricular treatment × time, $F_{(20,140)} = 1.927$, $p < 0.05$; repeated ANOVA) (Fig. 6*B*). The levels of basal DA did not differ among the three groups.

Next, we examined the *in vivo* effect of shati-AS on [^{3}H]DA uptake into synaptosomes in the midbrain. The experimental schedule is shown in Figure 6*C*. METH decreased [^{3}H]DA uptake compared with the saline-treated mice. In shati-AS-treated mice, the METH-induced decrease in [^{3}H]DA uptake was significantly potentiated compared with that in the shati-SC- or CSF-treated mice. Moreover, [^{3}H]DA uptake in the saline-treated group was also decreased by shati-AS compared with that in the shati-SC- or CSF-treated mice, although shati-SC had no effect on [^{3}H]DA uptake (drug, $F_{(1,40)} = 30.447$, $p < 0.01$; intracerebroventricular treatment, $F_{(2,40)} = 12.576$, $p < 0.01$; drug × intracerebroventricular treatment, $F_{(2,40)} = 0.392$, $p = 0.678$; two-way ANOVA) (Fig. 6*D*).

We also examined the *in vivo* effect of shati-AS on [^{3}H]DA uptake into synaptic vesicle preparations in the midbrain, because the redistribution of DA from synaptic vesicles to cytoplasmic compartments through interaction with vesicular monoamine transporter-2 has been postulated to be primarily responsible for DA terminal injury by METH or amphetamines (Liu and Edwards, 1997; Uhl, 1998). METH decreased vesicular [^{3}H]DA uptake compared with the saline-treated mice. In shati-AS-treated mice, the METH-induced decrease in vesicular [^{3}H]DA uptake was significantly potentiated compared with that in the shati-SC- or CSF-treated mice. Moreover, [^{3}H]DA uptake in the saline-treated group was also decreased by shati-AS compared with that in the shati-SC- or CSF-treated mice, although shati-SC had no effect on [^{3}H]DA uptake (drug, $F_{(1,42)} = 137.229$, $p < 0.01$; intracerebroventricular treatment, $F_{(2,42)} = 15.087$, $p < 0.01$; drug × intracerebroventricular treatment, $F_{(2,42)} = 0.240$, $p = 0.788$; two-way ANOVA) (Fig. 6*E*).

Different results were obtained from *in vivo* microdialysis and DA uptake studies, only in the basal conditions. These studies were performed in quite different situations. Living mice were used *in vivo* microdialysis study, and basal overflow of endogenous DA was measured 24 h after the last METH treatment in the NAc (Fig. 6*B*). Therefore, other factors (other neurotransmitters, neuroplasticity, and neuronal input from other brain regions) might affect basal DA overflow and compensate the dysfunction of DA uptake induced by repeated treatment of METH. Conversely, the experiment of [^{3}H]DA uptake was *ex vivo* study by using the midbrain tissue (Fig. 6*D*,*E*). High-concentration and exogenous [^{3}H]DA was used for the investigation of functional changes of DA uptake 1 h after the last METH treatment in the midbrain. The *ex vivo* method could more directly measure the changes of DA uptake in the midbrain, comparing *in vivo* microdialysis study.

Roles of shati in METH-induced conditioned place preference

The effect of shati-AS on METH-induced CPP was examined in a place conditioning paradigm, in which animals learn the association of an environment paired with drug exposure. This paradigm involves sensory perception of external stimuli, association of stimuli, and the approach-inducing actions of a drug, as well as the rewarding effects of a drug. The experimental schedule is shown in Figure 7*A*. As shown in Figure 7*B*, METH (0.3 mg/kg, s.c.) produced place preference in mice. In shati-AS-treated mice, the development of METH-induced CPP was significantly potentiated compared with that in the shati-SC- or CSF-treated mice (drug, $F_{(1,46)} = 78.202$, $p < 0.01$; intracerebroventricular treatment, $F_{(2,46)} = 4.950$, $p = 0.011$; drug × intracerebroventricular treatment, $F_{(2,46)} = 5.046$, $p = 0.010$; two-way ANOVA) (Fig. 7*B*), indicating that downregulation of shati expression was sufficient to confer the enhanced METH-induced CPP. Shati-AS, shati-SC, or CSF treatment had no effect on CPP in saline-treated mice (Fig. 7*B*, left three columns), suggesting that the procedure in CPP might not reflect anxiolytic actions. These results suggest that shati participates in the repeated METH treatment-induced development of behavioral sensitization and CPP by regulating DA uptake.

Discussion

In the present study, we identified a novel molecule shati from the NAc of mice treated with METH for the first time using the PCR-select cDNA subtraction method, which is a differential and epochal cloning technique.

From motif analysis of shati, shati contained the sequence of GCAT (Fig. 1*C*). Shati might have physiological action in producing acetylcholine or metabolic action of ATP, because the analysis showed the lowest interactive potential energy of shati with acetyl-CoA or ATP (supplemental Fig. 2, available at www.jneurosci.org as supplemental material). Accordingly, we have to investigate the mechanism by which shati regulates production of acetylcholine or metabolic roles of ATP in subsequent studies.

Because shati expression was detected at high levels in not only the brain regions related to drug dependence but also the liver, kidney, and spleen (Fig. 2*A*), it is plausible that shati is involved in the regulation of pathophysiological function. Single METH treatment induced the expression of shati mRNA in the NAc and Hip (Fig. 3*C*). Repeated METH treatment produces an enhancement of the locomotor-stimulating effects of METH (data not shown). Remarkable induction of shati mRNA expression was detected in the Fc, NAc, and CPu of the mice that

←

after METH treatment on the day 3. Values are means ± SE ($n = 8$). $^*p < 0.05$ versus saline-treated mice. $^\#p < 0.05$ versus shati-SC-treated mice. *C*, Experimental schedule for measurement of locomotor activity using shati-AS. *D*, Effect of shati-AS on repeated METH-induced behavioral sensitization. Mice were administered METH (1 or 2 mg/kg, s.c.) or saline for 5 d and challenged with METH (0.3 mg/kg, s.c.) on day 10. Locomotor activity was measured for 2 h on the days 1, 3, 5, and 10. Values are means ± SE ($n = 5$–7). ANOVA with repeated measures revealed significant differences in METH-induced sensitization (group, $F_{(8,47)} = 51.238$, $p < 0.01$; day, $F_{(2,94)} = 68.423$, $p < 0.01$; group × day, $F_{(16,94)} = 4.412$, $p < 0.01$). $^*p < 0.05$ versus METH plus CSF-treated mice. $^\#p < 0.05$ versus METH plus shati-SC-treated mice. $^\$p < 0.05$ versus the locomotor activity on day 1 in the same group.

showed behavioral sensitization to METH (Fig. 3*A–C*). There is strong evidence that the dopaminergic system, which projects from the VTA of the midbrain to the NAc and to other forebrain sites, including the Fc, dorsal striatum, and Hip, is a major substrate of reward and reinforcement for both natural rewards and addictive drugs (Di Chiara and Imperato, 1988; Robbins and Everitt, 1996; Wise, 1996a). Therefore, shati may be involved in the rewarding effects and reinforcement of addictive drugs. Because the dopaminergic neuronal system is involved primarily in the pharmacological effects of METH (Melega et al., 1995; Larsen et al., 2002; Sulzer et al., 2005), we examined whether the METH-induced increase in shati mRNA levels is mediated by the activation of dopaminergic neurotransmission. The METH-induced increase in the expression of shati mRNA in the NAc was completely inhibited by pretreatment with the DA D_1-like receptor antagonist *R*(+)-SCH23390 and the DA D_2-like receptor antagonist raclopride (Fig. 3*D*), suggesting that the activation of DA D_1 and D_2 receptors is attributable to METH-induced expression of shati. Behavioral studies have suggested that both DA D_1 and D_2 receptors mediate reinforcing signals for drug of abuse, because amphetamine-induced CPP and METH-induced sensitization are blocked by either DA D_1-like or D_2-like receptor antagonist (Ujike et al., 1989; Hiroi and White, 1991). Therefore, it likely that activation of DA transmission is necessary for METH-induced shati expression in neurons, in which shati specifically acts (Fig. 4*A*).

The contribution of dopaminergic transmission to behavioral sensitization and CPP has been well documented (Nakajima et al., 2004; Nagai et al., 2005a,b; Niwa et al., 2007a,b,d). Shati expression was upregulated by repeated administration of METH (Figs. 2*B*, 3, 4*A*), and downregulation of shati by AS (Figs. 4*B*, 5*B*) led to an elevated synaptic DA concentration in the NAc and major behavioral manifestations in mice: heightened locomotor activity (Fig. 5*D*), the rate of development of sensitization (Fig. 5*D*), and CPP (Fig. 7*B*) responding to METH. Furthermore, downregulation of shati expression by AS (Figs. 4*B*, 5*B*) potentiated the effects of METH on overflow of DA in the NAc (Fig. 6*B*) and DA uptake (Fig. 6*D*,*E*). These findings strongly suggest that the overexpression of shati elicited by METH may serve as a homeostatic mechanism that prevents hyperlocomo-

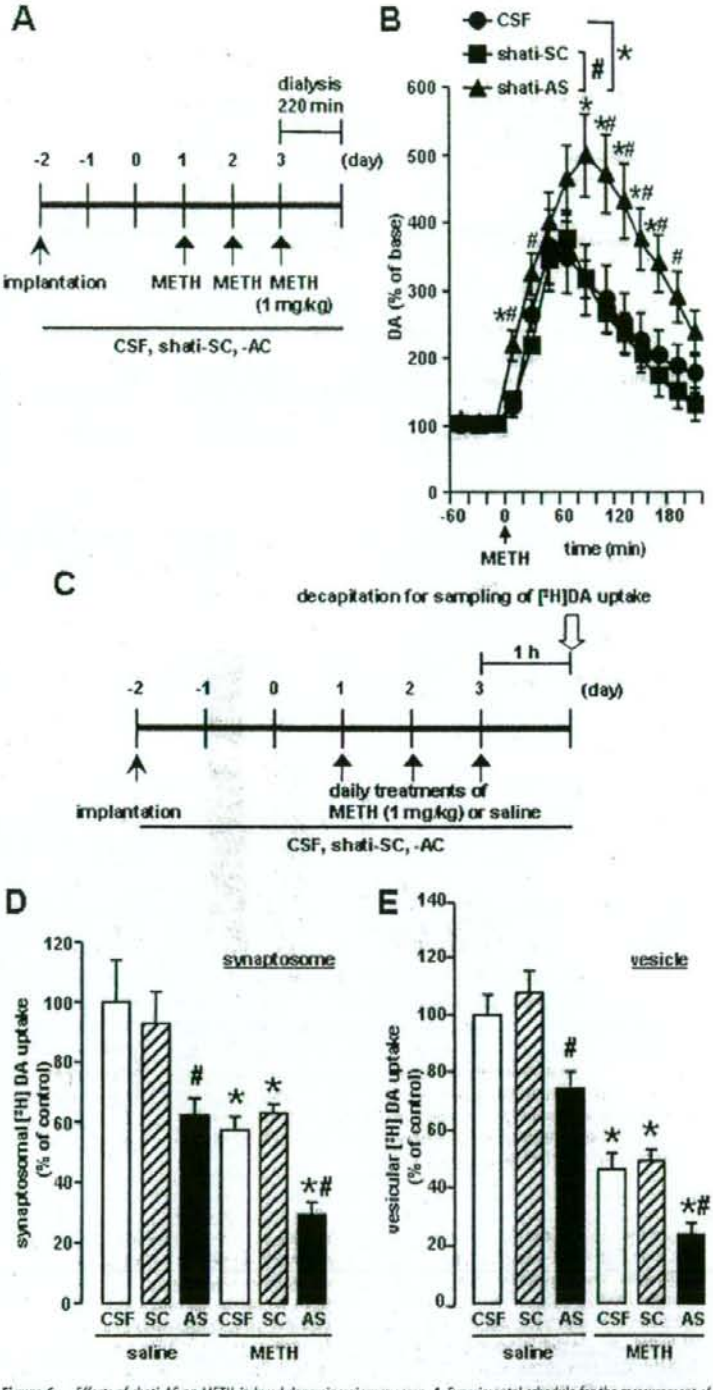

Figure 6. Effects of shati-AS on METH-induced dopaminergic responses. *A*, Experimental schedule for the measurement of overflow of DA using *in vivo* microdialysis using shati-AS. *B*, Effect of shati-AS on METH-induced increase in overflow of DA in the NAc. Mice were administered METH (1 mg/kg, s.c.) for 3 d. On day 3, levels of DA were measured in the NAc (AP +1.7 mm, ML −0.8 mm from bregma, and DV −4.0 mm from the skull) for 220 min after METH treatment by *in vivo* microdialysis. Basal levels of DA were 0.30 ± 0.08, 0.31 ± 0.05, and 0.30 ± 0.04 nM for the CSF-treated, shati-SC-treated, and shati-AS-treated mice, respectively. ANOVA with repeated measures revealed significant differences in METH-induced increase in overflow of DA (group,

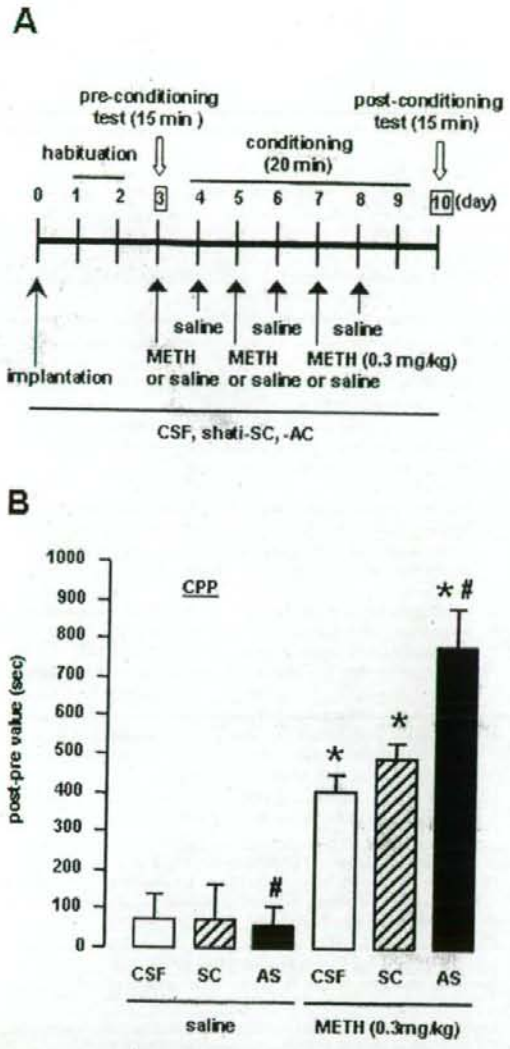

Figure 7. Effects of shati-AS on METH-induced conditioned place preference. ***A***, Experimental schedule for the conditioned place preference task using shati-AS. ***B***, Effect of shati-AS on METH-induced place preference. Mice were administered METH (0.3 mg/kg, s.c.) or saline during the conditioning for place preference. Values are means ± SE ($n = 5–12$). $^{*}p < 0.05$ versus saline-treated mice. $^{\#}p < 0.05$ versus shati-SC-treated mice.

←

$F_{(2,14)} = 5.662, p < 0.05$; time, $F_{(10,140)} = 35.646, p < 0.01$; group × time, $F_{(20,140)} = 1.927, p < 0.05$). Values are means ± SE ($n = 5–6$). $^{*}p < 0.05$ versus CSF-treated mice. $^{\#}p < 0.05$ versus shati-SC-treated mice. ***C***, Experimental schedule for the [^{3}H]DA uptake assay using shati-AS. ***D***, Effect of shati-AS on METH-induced decrease of synaptosomal [^{3}H]DA uptake. Mice were administered METH (1 mg/kg, s.c.) for 3 d and decapitated 1 h after the last injection. The synaptosomal [^{3}H]DA uptake was 0.32 ± 0.04, 0.29 ± 0.03, 0.20 ± 0.02, 0.18 ± 0.01, 0.20 ± 0.01, and 0.09 ± 0.01 pmol/mg protein per 4 min for the saline plus CSF-treated, saline plus shati-SC-treated, saline plus shati-AS-treated, METH plus CSF-treated, METH plus shati-SC-treated, and METH plus shati-AS-treated mice, respectively. The final concentration of [^{3}H]DA was 5 nM. Values are means ± SE ($n = 7–8$). $^{*}p < 0.05$ versus saline-treated mice. $^{\#}p < 0.05$ versus shati-SC-treated mice. ***E***, Effect of shati-AS on METH-induced decrease of vesicular [^{3}H]DA uptake. Mice were administered METH (1 mg/kg, s.c.) for 3 d and decapitated 1 h after the last injection. The vesicular [^{3}H]DA uptake was 3.76 ± 0.25, 4.05 ± 0.29, 2.80 ± 0.20, 1.74 ± 0.21, 1.85 ± 0.14, and 0.90 ± 0.14 pmol/mg protein per 4 min for the saline plus CSF-treated, saline plus shati-SC-treated, saline plus shati-AS-treated, METH plus CSF-treated, METH plus shati-SC-treated, and METH plus shati-AS-treated mice, respectively. The final concentration of [^{3}H]DA was 30 nM. Values are means ± SE ($n = 8$). $^{*}p < 0.05$ versus saline-treated mice. $^{\#}p < 0.05$ versus shati-SC-treated mice.

tion, sensitization, and CPP, by promoting plasmalemmal and vesicular DA uptake as well as attenuating the METH-induced increase in overflow of DA in the NAc.

We used METH at the dose of 2 mg/kg for 6 d in the experiments of RT-PCR, real-time RT-PCR, and immunohistochemistry (Figs. 3, 4*B–D*, 5), because expression of shati was induced in the NAc of mice by METH (2 mg/kg for 6 d), which was detected by using a PCR-select cDNA subtraction method (supplemental Fig. 1, available at www.jneurosci.org as supplemental material). In AS experiments, shati-AS-treated mice tended to show a potentiation of METH (2 mg/kg)-induced hyperlocomotion and sensitization on days 1–5, but there were no statistically significant differences among the three groups (Fig. 5*D*). The dose–response effects of METH on the locomotor activity may reflect a shift to the left, but these effects were reached the plateau. Conversely, shati-AS-treated mice showed a marked potentiation of METH (1 mg/kg)-induced hyperlocomotion and sensitization on days 1–5 compared with shati-SC- or CSF-treated mice (Fig. 5*D*). On day 3, the potentiation of the METH-induced hyperlocomotion by shati-AS reached the maximum and plateau. Therefore, in the experiments of AS, we selected METH at the dose of 1 mg/kg for 3 d (Figs. 5*B*, 6*B*,*D*,*E*). We also confirmed that shati mRNA was increased by METH at the doses of 1 and 2 mg/kg for 3 d (Fig. 3*A*). Then, in the AS study, we selected METH at the dose of 1 mg/kg to investigate effects of AS.

We selected the time point of 2 h after the last METH treatment for the time when the animals were to be killed in the experiments of RT-PCR and real-time RT-PCR (Figs. 2, 3*A*,*C*,*D*), because expression of shati mRNA showed peak in the NAc of mice 2 h after the last METH treatment (Fig. 3*B*). We prepared the brain samples 24 h after the last METH treatment for immunohistochemical study (Fig. 4). The levels of shati mRNA in the NAc of mice treated with repeated METH were significantly increased 2, 6, and 24 h after the last METH treatment (Fig. 3*B*). At 24 h after the METH treatment, both transcription and translation of shati protein could be induced in the brain. Therefore, we considered that 24 h after the METH treatment is the best time point for investigation of shati protein expression.

Changes in mRNA and protein expression caused by drugs are of particular interest. The expression of certain mRNAs and proteins appears to be a compensatory adaptation to excessive DA signaling, which could be biologically significant adaptive mechanisms contributing to dependence. Nevertheless, some proteins play a reverse role. For example, we previously demonstrated that tPA potentiates METH- or MOR-induced rewarding and locomotor-stimulating effects (Nagai et al., 2004, 2005a,b), whereas TNF-α and its inducer inhibit them (Nakajima et al., 2004; Niwa et al., 2007a,b,d). The development of sensitization to amphetamine is prevented when an antibody that neutralized basic fibroblast growth factor (bFGF) is infused into the VTA before amphetamine treatment (Flores et al., 2000). Infusion of brain-derived neurotrophic factor (BDNF) into the NAc enhances the stimulation of locomotor activity by cocaine in rats, whereas the development of sensitization and CPP is delayed in heterozygous BDNF knock-out mice compared with wild-type littermates (Horger et al., 1999; Hall et al., 2003). Infusion of GDNF into the VTA blocks certain biochemical adap-

tations to chronic cocaine treatment (induction of tyrosine hydroxylase, NR1 subunit of NMDA receptors, ΔFosB, and protein kinase A catalytic subunit) as well as cocaine-induced rewarding effects (Messer et al., 2000). Conversely, responses to cocaine are enhanced in rats by intra-VTA infusion of anti-GDNF antibody and in GDNF heterozygous knock-out mice (Messer et al., 2000). A partial reduction in the expression of GDNF potentiates METH self-administration, enhances motivation to take METH, increases vulnerability to drug-primed reinforcement, and prolongs cue-induced reinforcement of extinguished METH-seeking behavior (Yan et al., 2007). cAMP response element-binding protein (CREB) overexpression in the NAc reduces the rewarding properties of cocaine, whereas expression of a dominant-negative form of CREB in this region has the opposite effect (Carlezon et al., 1998; Walters and Blendy, 2001; McClung and Nestler, 2003). Furthermore, *Fos*B mutant mice shows exaggerated locomotor activation in response to initial cocaine exposures as well as robust CPP to a lower dose of cocaine compared with wild-type littermates (Hiroi et al., 1997). Changes in the balance of levels between proaddictive factors, such as bFGF, tPA, and BDNF, and anti-addictive factors, such as TNF-α, GDNF, CREB, and *Fos*B, induced by drugs of abuse seems to be important to the development of drug dependence. In the present study, the facilitation of METH-induced behavioral sensitization in mice with a targeted downregulation of shati highlights the opposing role of shati in drug-dependent behavioral plasticity. Therefore, upregulation of shati expression may represent a homeostastatic response of dopaminergic neurons in the NAc to excessive dopaminergic transmission, resulting in attenuation of hypersensitivity and CPP induced by METH-like drugs. Our findings, together with others, suggest that there are molecules in the brain that normally inhibit the behavioral actions of addictive substances. The mechanism underlying the upregulation of shati caused by METH remains to be elucidated; nevertheless, inhibitory feedback of the excessive DA signaling is likely to be a plausible candidate.

In conclusion, the present study established a functional interaction between shati and METH. Our findings suggest that shati is involved in the development of METH-induced hyperlocomotion, sensitization, and CPP, by promoting plasmalemmal and vesicular DA uptake as well as attenuating the METH-induced increase in overflow of DA in the NAc.

References

Ang E, Chen J, Zagouras P, Magna H, Holland J, Schaeffer E, Nestler EJ (2001) Induction of nuclear factor-κB in nucleus accumbens by chronic cocaine administration. J Neurochem 79:221–224.

Blackshaw S, Harpavat S, Trimarchi J, Cai L, Huang H, Kuo WP, Weber G, Lee K, Fraioli RE, Cho SH, Yung R, Asch E, Ohno-Machado L, Wong WH, Cepko CL (2004) Genomic analysis of mouse retinal development. PLoS Biol 2:E247.

Bowers MS, McFarland K, Lake RW, Peterson YK, Lapish CC, Gregory ML, Lanier SM, Kalivas PW (2004) Activator of G protein signaling 3: a gatekeeper of cocaine sensitization and drug seeking. Neuron 42:269–281.

Carlezon Jr WA, Thome J, Olson VG, Lane-Ladd SB, Brodkin ES, Hiroi N, Duman RS, Neve RL, Nestler EJ (1998) Regulation of cocaine reward by CREB. Science 282:2272–2275.

Cha XY, Pierce RC, Kalivas PW, Mackler SA (1997) NAC-1, a rat brain mRNA, is increased in the nucleus accumbens three weeks after chronic cocaine self-administration. J Neurosci 17:6864–6871.

Christensen AV, Arnt J, Hyttel J, Larsen JJ, Svendsen O (1984) Pharmacological effects of a specific dopamine D-1 antagonist SCH 23390 in comparison with neuroleptics. Life Sci 34:1529–1540.

Diatchenko L, Lau YF, Campbell AP, Chenchik A, Moqadam F, Huang B, Lukyanov S, Lukyanov K, Gurskaya N, Sverdlov ED, Siebert PD (1996) Suppression subtractive hybridization: a method for generating differentially regulated or tissue-specific cDNA probes and libraries. Proc Natl Acad Sci USA 93:6025–6030.

Di Chiara G, Imperato A (1988) Drugs abused by humans preferentially increase synaptic dopamine concentrations in the mesolimbic system of freely moving rats. Proc Natl Acad Sci USA 85:5274–5278.

Douglass J, Daoud S (1996) Characterization of the human cDNA and genomic DNA encoding CART: a cocaine- and amphetamine-regulated transcript. Gene 169:241–245.

Erickson JD, Masserano JM, Barnes EM, Ruth JA, Weiner N (1990) Chloride ion increases [^{3}H]dopamine accumulation by synaptic vesicles purified from rat striatum: inhibition by thiocyanate ion. Brain Res 516:155–160.

Fleckenstein AE, Metzger RR, Wilkins DG, Gibb JW, Hanson GR (1997) Rapid and reversible effects of methamphetamine on dopamine transporters. J Pharmacol Exp Ther 282:834–838.

Flores C, Samaha AN, Stewart J (2000) Requirement of endogenous basic fibroblast growth factor for sensitization to amphetamine. J Neurosci 20:RC55(1–5).

Franklin KBJ, Paxinos G (1997) The mouse brain: in stereotaxic coordinates. San Diego: Academic.

Giros B, Jaber M, Jones SR, Wightman PM, Caron MG (1996) Hyperlocomotion and indifference to cocaine and amphetamine in mice lacking the dopamine transporter. Nature 379:606–612.

Gurskaya NG, Diatchenko L, Chenchik A, Siebert PD, Khaspekov GL, Lukyanov KA, Vagner LL, Ermolaeva OD, Lukyanov SA, Sverdlov ED (1996) Equalizing cDNA subtraction based on selective suppression of polymerase chain reaction: cloning of Jurkat cell transcripts induced by phytohemaglutinin and phorbol 12-myristate 13-acetate. Anal Biochem 240:90–97.

Hall FS, Drgonova J, Goeb M, Uhl GR (2003) Reduced behavioral effects of cocaine in heterozygous brain-derived neurotropic factor (BDNF) knockout mice. Neuropsychopharmacology 28:1485–1490.

Heikkila RE, Orlansky H, Cohen G (1975) Studies on the distinction between uptake inhibition and release of ^{3}H-dopamine in rat brain tissue slices. Biochem Pharmacol 24:847–852.

Hiroi N, White NM (1991) The amphetamine conditioned place preference: differential involvement of dopamine receptor subtypes and two dopaminergic terminal areas. Brain Res 552:141–152.

Hiroi N, Brown JR, Haile CN, Ye H, Greenberg ME, Nestler EJ (1997) FosB mutant mice: loss of chronic cocaine induction of Fos-related proteins and heightened sensitivity to cocaine's psychomotor and rewarding effects. Proc Natl Acad Sci USA 94:10397–10402.

Horger BA, Iyasere CA, Berhow MT, Messer CJ, Nestler EJ, Taylor JR (1999) Enhancement of locomotor activity and conditioned reward to cocaine by brain-derived neurotropic factor. J Neurosci 19:4110–4122.

Koob GF (1992) Drugs of abuse: anatomy, pharmacology and function of reward pathways. Trends Pharmacol Sci 13:177–184.

Koob GF, Sanna PP, Bloom FE (1998) Neuroscience of addiction. Neuron 21:467–476.

Laakso A, Mohn AR, Gainetdinov RR, Caron MG (2002) Experimental genetic approaches to addiction. Neuron 36:213–228.

Larsen KE, Fon EA, Hastings TG, Edwards RH, Sulzer D (2002) Methamphetamine-induced degeneration of dopaminergic neurons involves autophagy and upregulation of dopamine synthesis. J Neurosci 22:8951–8960.

Liu Y, Edwards RH (1997) The role of vesicular transporter proteins in synaptic transmission and neural degeneration. Annu Rev Neurosci 20:125–156.

Lorrain DS, Arnold GM, Vezina P (2000) Previous exposure to amphetamine increases incentive to obtain the drug: long-lasting effects revealed by the progressive ratio schedule. Behav Brain Res 107:9–19.

McClung CA, Nestler EJ (2003) Regulation of gene expression and cocaine reward by CREB and ΔFosB. Nat Neurosci 6:1208–1215.

Melega WP, Williams AE, Schmitz DA, DiStefano EW, Cho AK (1995) Pharmacokinetic and pharmacodynamic analysis of the actions of D-amphetamine and D-methamphetamine on the dopamine terminal. J Pharmacol Exp Ther 274:90–96.

Messer CJ, Eisch AJ, Carlezon Jr WA, Whisler K, Shen L, Wolf DH, Westphal H, Collins F, Russell DS, Nestler EJ (2000) Role for GDNF in biochemical and behavioral adaptations to drugs of abuse. Neuron 26:247–257.

Mizoguchi H, Yamada K, Mizuno M, Mizuno T, Nitta A, Noda Y, Nabeshima T (2004) Regulations of methamphetamine reward by extracellular

signal-regulated kinase 1/2/ets-like gene-1 signaling pathway via the activation of dopamine receptors. Mol Pharmacol 65:1293–1301.
Mizoguchi H, Yamada K, Niwa M, Mouri A, Mizuno T, Noda Y, Nitta A, Itohara S, Banno Y, Nabeshima T (2007) Reduction of methamphetamine-induced sensitization and reward in matrix metalloproteinase-2 and -9-deficient mice. J Neurochem 100:1579–1588.
Nagai T, Yamada K, Yoshimura M, Ishikawa K, Miyamoto Y, Hashimoto K, Noda Y, Nitta A, Nabeshima T (2004) The tissue plasminogen activator-plasmin system participates in the rewarding effect of morphine by regulating dopamine release. Proc Natl Acad Sci USA 101:3650–3655.
Nagai T, Noda Y, Ishikawa K, Miyamoto Y, Yoshimura M, Ito M, Takayanagi M, Takuma K, Yamada K, Nabeshima T (2005a) The role of tissue plasminogen activator in methamphetamine-related reward and sensitization. J Neurochem 92:660–667.
Nagai T, Kamei H, Ito M, Hashimoto K, Takuma K, Nabeshima T, Yamada K (2005b) Modification by the tissue plasminogen activator-plasmin system of morphine-induced dopamine release and hyperlocomotion, but not anti-nociceptive effect in mice. J Neurochem 93:1272–1279.
Nagai T, Ito M, Nakamichi N, Mizoguchi H, Kamei H, Fukakusa A, Nabeshima T, Takuma K, Yamada K (2006) The rewards of nicotine: regulation by tissue plasminogen activator-plasmin system through protease activated receptor-1. J Neurosci 26:12374–12383.
Nakajima A, Yamada K, Nagai T, Uchiyama T, Miyamoto Y, Mamiya T, He J, Nitta A, Mizuno M, Tran MH, Seto A, Yoshimura M, Kitaichi K, Hasegawa T, Saito K, Yamada Y, Seishima M, Sekikawa K, Kim HC, Nabeshima T (2004) Role of tumor necrosis factor-α in methamphetamine-induced drug dependence and neurotoxicity. J Neurosci 24:2212–2225.
Napier TC, Givens BS, Schulz DW, Bunney BS, Breese GR, Mailman RB (1986) SCH23390 effects on apomorphine-induced responses of nigral dopaminergic neurons. J Pharmacol Exp Ther 236:838–845.
Nestler EJ (2001) Molecular basis of long-term plasticity underlying addiction. Nat Rev Neurosci 2:119–128.
Nestler EJ (2002) From neurobiology to treatment: progress against addiction. Nat Neurosci 5:1076–1079.
Niwa M, Nitta A, Shen L, Noda Y, Nabeshima T (2007a) Involvement of glial cell line-derived neurotrophic factor in inhibitory effects of a hydrophobic dipeptide Leu-Ile on morphine-induced sensitization and rewarding effects. Behav Brain Res 179:167–171.
Niwa M, Nitta A, Yamada Y, Nakajima A, Saito K, Seishima M, Shen L, Noda Y, Furukawa S, Nabeshima T (2007b) An inducer for glial cell line-derived neurotrophic factor and tumor necrosis factor-α protects against methamphetamine-induced rewarding effects and sensitization. Biol Psychiatry 61:890–901.
Niwa M, Nitta A, Yamada K, Nabeshima T (2007c) The roles of glial cell line-derived neurotrophic factor, tumor necrosis factor-α, and an inducer of these factors in drug dependence. J Pharmacol Sci, in press.
Niwa M, Nitta A, Yamada Y, Nakajima A, Saito K, Seishima M, Noda Y, Nabeshima T (2007d) Tumor necrosis factor-α and its inducer inhibit morphine-induced rewarding effects and sensitization. Biol Psychiatry, in press.
Noda Y, Miyamoto Y, Mamiya T, Kamei H, Furukawa H, Nabeshima T (1998) Involvement of dopaminergic system in phencyclidine-induced place preference in mice pretreated with phencyclidine repeatedly. J Pharmacol Exp Ther 286:44–51.
Robbins TW, Everitt BJ (1996) Neurobehavioural mechanisms of reward and motivation. Curr Opin Neurobiol 6:228–236.
Robinson TE, Berridge KC (1993) The neural basis of drug craving: an incentive-sensitization theory of addiction. Brain Res Brain Res Rev 18:247–291.
Satel SL, Southwick SM, Gawin FH (1991) Clinical features of cocaine-induced paranoia. Am J Psychiatry 148:495–498.
Schechter MD, Calcagnetti DJ (1998) Continued trends in the conditioned place preference literature from 1992 to 1996, inclusive, with a cross-indexed bibliography. Neurosci Biobehav Rev 22:827–846.
Seiden LS, Sabol KE, Ricaurte GA (1993) Amphetamine: effects on catecholamine systems and behavior. Annu Rev Pharmacol Toxicol 33:639–677.
Strakowski SM, Sax KW (1998) Progressive behavioral response to repeated d-amphetamine challenge: further evidence for sensitization in humans. Biol Psychiatry 44:1171–1177.
Strausberg RL, Feingold EA, Grouse LH, Derge JG, Klausner RD, Collins FS, Wagner L, Shenmen CM, Schuler GD, Altschul SF, Zeeberg B, Buetow KH, Schaefer CF, Bhat NK, Hopkins RF, Jordan H, Moore T, Max SI, Wang J, Hsieh F et al. (2002) Generation and initial analysis of more than 15,000 full-length human and mouse cDNA sequences. Proc Natl Acad Sci USA 99:16899–16903.
Sulzer D, Sonders MS, Poulsen NW, Galli A (2005) Mechanisms of neurotransmitter release by amphetamines: a review. Prog Neurobiol 75:406–433.
Taubenfeld SM, Milekic MH, Monti B, Alberini CM (2001) The consolidation of new but not reactivated memory requires hippocampal C/EBPβ. Nat Neurosci 4:813–818.
Uhl GR (1998) Hypothesis: the role of dopaminergic transporters in selective vulnerability of cells in Parkinson's disease. Ann Neurol 43:555–560.
Ujike H, Onoue T, Akiyama K, Hamamura T, Otsuki S (1989) Effects of selective D-1 and D-2 dopamine antagonists on development of methamphetamine-induced behavioral sensitization. Psychopharmacology 98:89–92.
Wada R, Tifft CJ, Proia RL (2000) Microglial activation precedes acute neurodegeneration in Sandhoff disease and is suppressed by bone marrow transplantation. Proc Natl Acad Sci USA 97:10954–10959.
Walters CL, Blendy JA (2001) Different requirements for cAMP response element binding protein in positive and negative reinforcing properties of drugs of abuse. J Neurosci 21:9438–9444.
Wang XB, Funada M, Imai Y, Revay RS, Ujike H, Vandenbergh DJ, Uhl GR (1997) rGβ1: a psychostimulant-regulated gene essential for establishing cocaine sensitization. J Neurosci 17:5993–6000.
Wise RA (1996a) Addictive drugs and brain stimulation reward. Annu Rev Neurosci 19:319–340.
Wise RA (1996b) Neurobiology of addiction. Curr Opin Neurobiol 6:243–251.
Wolf ME (1998) The role of excitatory amino acids in behavioral sensitization to psychomotor stimulants. Prog Neurobiol 54:679–720.
Yamada K, Nabeshima T (2004) Pro- and anti-addictive neurotrophic factors and cytokines in psychostimulant addiction: mini review. Ann NY Acad Sci 1025:198–204.
Yan Y, Yamada K, Niwa M, Nagai T, Nitta A, Nabeshima T (2007) Enduring vulnerability to reinstatement of methamphetamine-seeking behavior in glial cell line-derived neurotrophic factor mutant mice. FASEB J, in press.
Zachariou V, Bolanos CA, Selley DE, Theobald D, Cassidy MP, Kelz MB, Shaw-Lutchman T, Berton O, Sim-Selley LJ, Dileone RJ, Kumar A, Nestler EJ (2006) An essential role for ΔFosB in the nucleus accumbens in morphine action. Nat Neurosci 9:205–211.

JPP Journal of Pharmacy and Pharmacology

JPP 2007, 59: 1383–1387
© 2007 The Authors
Received March 28, 2007
Accepted July 6, 2007
DOI 10.1211/jpp.59.10.0008
ISSN 0022-3573

Carvedilol increases ciclosporin bioavailability by inhibiting P-glycoprotein-mediated transport

Katsuo Amioka, Takafumi Kuzuya, Hideyuki Kushihara, Masayuki Ejiri, Atsumi Nitta and Toshitaka Nabeshima*

Abstract

Carvedilol is often used to treat hypertension and for prophylaxis in vascular sclerosis in renal transplant recipients, who require concomitant treatment with ciclosporin. However, there are few reports regarding the pharmacokinetic interactions between carvedilol and ciclosporin. We have investigated the potential effects of carvedilol on the pharmacokinetics of ciclosporin, and examined the inhibitory effects of carvedilol on P-glycoprotein-mediated transcellular transport using Caco2 cells. Ciclosporin alone or with carvedilol was orally or intravenously administered to rats. The oral administration of carvedilol (10 mg kg^{-1}) with ciclosporin (10 mg kg^{-1}) increased the whole blood concentration of ciclosporin. When ciclosporin (3 mg kg^{-1}) was intravenously administered with carvedilol (3 mg kg^{-1}), there was no difference in the whole blood ciclosporin concentration between administration with and without carvedilol. Co-administration with carvedilol increased ciclosporin bioavailability from 33% to 70%. In Caco2 cells, carvedilol caused a concentration-dependent increase in the intracellular accumulation of ciclosporin, and its effect was comparable with that of verapamil. Carvedilol considerably raised the concentration of ciclosporin in the blood and this interaction was associated with the absorption phase of ciclosporin. This interaction was caused by the inhibition of P-glycoprotein-mediated transport by carvedilol in the intestine.

Department of Neuropsychopharmacology and Hospital Pharmacy, Nagoya University School of Medicine, 65 Tsuruma-cho, Showa-ku, Nagoya 466-8560, Japan

Katsuo Amioka, Takafumi Kuzuya, Masayuki Ejiri, Atsumi Nitta, Toshitaka Nabeshima

Clinical Pharmacy, College of Pharmacy, Kinjogakuin University, 2-1723 Omori, Moriyama-ku, Nagoya 463-8521, Japan

Katsuo Amioka

Department of Hospital Pharmacy, Japanese Red Cross Nagoya First Hospital, 3-35 Mitishita-cho, Nakamura-ku, Nagoya, 453-8511, Japan

Hideyuki Kushihara

Correspondence:
T. Nabeshima, Department of Neuropsychopharmacology and Hospital Pharmacy, Nagoya University School of Medicine, 65 Tsuruma-cho, Showa-ku, Nagoya 466-8560, Japan. E-mail: tnabeshi@med.nagoya-u.ac.jp

Funding: This study was supported in part by a grant from Japan Society for the Promotion of Science (No. 17923025, 2005).

Introduction

Carvedilol is a nonselective β-blocking agent which has vasodilating properties that are attributed mainly to its blocking activity at α_1-receptors. Since carvedilol is used in the treatment of mild to moderate hypertension and does not affect renal perfusion and filtration, it can be given to renal transplant recipients (Heitmann et al 2002). In addition, carvedilol has been found to inhibit the proliferation and migration of vascular smooth muscle cells (Patel et al 1995; Park et al 2006). This pharmacological effect may be useful for renal transplant recipients because chronic rejection is associated with the abnormal proliferation and migration of vascular smooth muscle, and fibrosis is a common feature of transplant vascular sclerosis (Ishii et al 2005). For these reasons, there are many cases where carvedilol and immunosuppressive agents could and should be used concomitantly.

Carvedilol, when absorbed orally, is extensively metabolized and then excreted primarily into the bile (Gehr et al 1999). Ciclosporin, the principal immunosuppressant used in organ transplant patients and employed to treat a variety of autoimmune diseases, is extensively metabolized in the liver and eliminated mainly by biliary excretion (Lindholm 1991). Both drugs have been shown to be transported by P-glycoprotein, which plays a significant role in the oral absorption and excretion of xenobiotics (Saeki et al 1993; Kakumoto et al 2003). These points should be taken into account when considering factors affecting drug–drug interactions, and specifically the pharmacokinetics of ciclosporin. Indeed, we have had firsthand experience of increased ciclosporin blood levels after administering carvedilol concomitantly to a renal transplant patient: the patient's AUC_{0-4}/dose increased 24%. However, there are few reports describing the pharmacokinetic interaction between carvedilol and ciclosporin, and the mechanisms behind the interaction are not clear.

The purpose of this study was to examine the potential effects of carvedilol on the pharmacokinetics of ciclosporin. Furthermore, the inhibitory effects of carvedilol on

P-glycoprotein-mediated transport were investigated using a human colon adenocarcinoma cell line.

Materials and Methods

Materials

Ciclosporin and carvedilol were kindly provided by Novartis Pharma K. K. (Tokyo, Japan) and Daiichi Pharmaceutical Co. Ltd (Tokyo, Japan), respectively. Verapamil, Dulbecco's modified Eagle medium (DMEM), fetal bovine serum, Triton X-100, and trypsin were purchased from Sigma-Aldrich (St Louis, MO). HEPES, penicillin, streptomycin, and nonessential amino acids were purchased from Gibco BRL (Grand Island, NY). All other chemicals used were of the highest purity available.

Animal study

All experiments were performed in accordance with the Guidelines for Animal Experiments of Nagoya University Graduate School of Medicine. Male Wistar rats (280–320 g; Japan SLC Inc., Shizuoka, Japan) were used for the pharmacokinetic study. Although food was withdrawn overnight before the experiment, rats were always allowed free access to water. One day before drug administration, the rats were anaesthetized with an intraperitoneal injection of sodium pentobarbital (25 mg kg^{-1}). A silastic catheter was inserted into the right jugular vein to allow the collection of blood samples and as a route for intravenous administration. Doses of ciclosporin either alone or with carvedilol were orally (ciclosporin 10 mg kg^{-1}; carvedilol 10 mg kg^{-1}) or intravenously (ciclosporin 3 mg kg^{-1}; carvedilol 3 mg kg^{-1}) administered. These dosage adjustments were required due to the poor absorption of ciclosporin (27 ± 18% (Ptachcinski et al 1985)). Oral administration was accomplished by inserting a water-lubricated curved blunt stainless-steel catheter into the oesophagus. Blood samples were collected using heparinized syringes at 1, 2, 4, 6, 8, and 12 h post-dose and were analysed for ciclosporin using a fluorescence polarization immunoassay with a TDX analyser (Abbott Laboratories, Chicago, IL). Ciclosporin blood concentrations were fitted to a one-compartment model with first-order absorption and elimination using Prism 4 for Windows software (GraphPAD Software Inc, San Diego, CA).

Cell culture and intracellular accumulation study

P-glycoprotein function was studied in the epithelial layer of a human colon adenocarcinoma cell line, Caco-2, which demonstrates a P-glycoprotein-dependent intestinal absorptive cell phenotype. Caco-2 cells at passage 40 were obtained from Riken Gene Bank (Tsukuba, Japan). They were cultured in DMEM containing 10% fetal bovine serum, 100 U mL^{-1} penicillin, 100 μg mL^{-1} streptomycin, and 100 μM nonessential amino acids. The adhesive cells were harvested at 80% confluence by exposure to a trypsin-EDTA solution (0.25% trypsin and 0.02% EDTA in a phosphate-buffered solution).

Intracellular accumulation was studied according to a procedure described by Zhu et al (2006). In brief, Caco-2 cells were seeded at a density of 1×10^5 cells mL^{-1}/well in 24-well plates, and the culture medium was changed every two days until the experiment was initiated. After reaching confluence, Caco-2 cells were pre-incubated at 37°C for 30 min with serum-free DMEM containing 25 mM HEPES, pH 7.4. Ciclosporin and either carvedilol or verapamil were added to the culture medium to a final concentration of 0.1 μM for ciclosporin, and 0.02, 0.2, 0.6, 2 or 20 μM for carvedilol and verapamil. The solution contained no more than 0.1% dimethyl sulfoxide, and was discarded after 90-min incubation. The cells were washed three times with ice-cold phosphate-buffered saline and permeabilized with a 1% Triton X-100-containing buffer. The ciclosporin concentrations in the buffer were analysed using the method described above but with a different calibration curve. The amount of ciclosporin in each sample was standardized, with the protein content determined using a BCA protein assay kit (Pierce, Rockford, IL). The degree of inhibition observed at the different carvedilol or verapamil concentrations was estimated based on a 50% inhibitory concentration (IC50) determined with an inhibitory sigmoid E_{max} model using non-linear regression curve fitting; the results were analysed using Prism 4 for Windows software (GraphPAD Software Inc, San Diego, CA).

Statistical analysis

All data are presented as the mean ± s.d. The individual differences of ciclosporin concentrations with and without carvedilol at each sampling time were performed using a Mann–Whitney U-test. The differences of each pharmacokinetic parameter were also established using the same test, with $P < 0.05$ being taken as significant. All statistical analyses were performed with StatView 4.5 (Abacus Concepts Inc., Berkeley, CA).

Results

Pharmacokinetic study

Figure 1 shows the whole blood concentration–time curves of ciclosporin after oral (ciclosporin 10 mg kg^{-1}, Figure 1A) and intravenous (ciclosporin 3 mg kg^{-1}, Figure 1B) administration, with and without carvedilol (i.v. 3 mg kg^{-1}; p.o. 10 mg kg^{-1}). Co-administration of carvedilol significantly ($P < 0.05$) increased the whole blood concentration of ciclosporin following oral administration. When ciclosporin was intravenously administered with carvedilol, there was no difference in the whole blood ciclosporin concentration to when administered without carvedilol. The pharmacokinetic parameters of ciclosporin with and without carvedilol are shown in Table 1. Co-administration of carvedilol resulted in a decrease in clearance (CL) and a 2-fold increase in AUC and C_{max} compared with administration of ciclosporin alone when the drugs were taken orally. The pharmacokinetic parameters (AUC and CL) were not altered when carvedilol was administered intravenously. Since the increase in AUC was linear with ciclosporin dose, co-administration with carvedilol showed

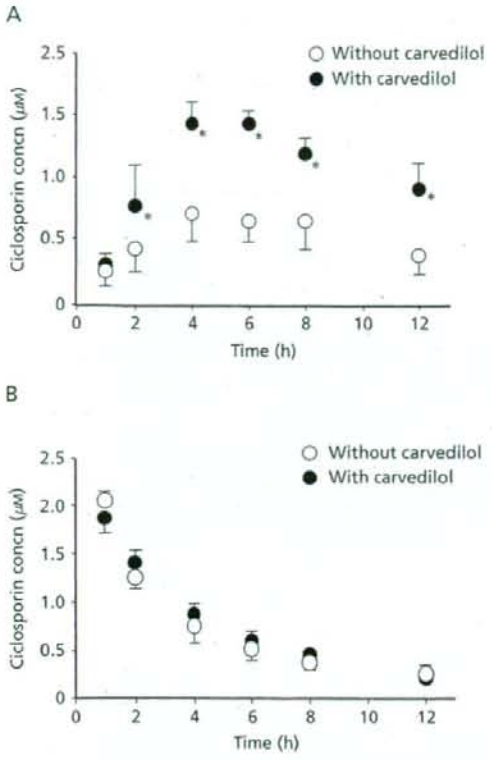

Figure 1 Whole blood concentration–time curves of ciclosporin after (A) 10 mg kg^{-1} orally administered with or without carvedilol or (B) 3 mg kg^{-1} intravenously administered with or without carvedilol. Each point represents the mean ± s.d. of four rats. *$P < 0.05$, significantly different from administration without carvedilol.

Table 1 Effect of carvedilol on pharmacokinetic parameters of ciclosporin

Parameter	Oral administration		Intravenous administration	
	Control	Carvedilol	Control	Carvedilol
AUC (μM h)	9.8 ± 2.7	23.6 ± 5.7	9.1 ± 1.7	10.2 ± 1.4
	$P < 0.01$		$P = 0.17$	
k_a (h^{-1})	0.17 ± 0.04	0.21 ± 0.06		
	$P = 0.38$			
k_{el} (h^{-1})	0.17 ± 0.06	0.17 ± 0.03	0.27 ± 0.08	0.23 ± 0.01
	$P = 0.46$		$P = 0.17$	
Vd/F (L kg^{-1})	4.25 ± 0.51	2.25 ± 0.13		
	$P < 0.01$			
Vd (L kg^{-1})			1.00 ± 0.40	1.10 ± 0.09
			$P = 0.47$	
CL/F (L h^{-1} kg^{-1})	0.71 ± 0.15	0.39 ± 0.03		
	$P < 0.01$			
CL (L h^{-1} kg^{-1})			0.27 ± 0.13	0.25 ± 0.03
			$P = 0.56$	
C_{max} (μM)	0.72 ± 0.10	1.42 ± 0.12		
	$P < 0.01$			

an increase in bioavailability of ciclosporin from 32.6% to 70.1%. The elimination rate constants were not altered by carvedilol administered either orally or intravenously. These results suggested that the increase in the AUC and C_{max} of ciclosporin induced by carvedilol via the oral route was mainly due to enhanced absorption of ciclosporin in the gastrointestinal tract, and not to inhibited elimination via the biliary tract or to hepatic metabolism.

Intracellular accumulation study

Ciclosporin is a substrate of P-glycoprotein and is transported across Caco-2 cell membranes. Since Caco-2 cells exhibit features typical of intestinal epithelial cells (Sambuy et al 2005), these cells have been used widely as a standard model for intestinal efflux, and for investigating the mechanisms of absorption of several classes of drugs. We evaluated the inhibitory effect of carvedilol on the efflux of ciclosporin using the intracellular accumulation study. As shown in Figure 2, the accumulation of ciclosporin was markedly increased in the presence of carvedilol, the effects of which were dependent on concentration. This concentration-dependent accumulation of ciclosporin was also found with verapamil in Caco-2 cells. The IC50 value of carvedilol (0.831 μM) was comparable with that of verapamil (0.616 μM).

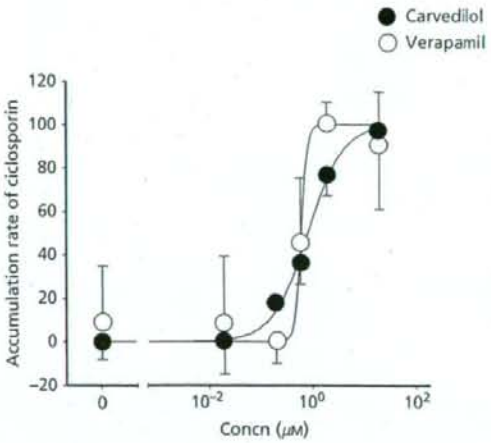

Figure 2 Concentration-dependent accumulation rate of 0.1 μM ciclosporin by carvedilol and verapamil in Caco-2 cells. The IC50 values of carvedilol and verapamil were 0.83 and 0.62 μM, respectively. Each point represents the mean ± s.d. of four data points.

Discussion

Padi & Chopra (2002) reported that ciclosporin induced oxidative stress and that the resultant renal dysfunction was prevented by carvedilol, which has potent antioxidative effects. These results indicated that co-administration of carvedilol

with ciclosporin was useful not only for the treatment of hypertension and the inhibition of muscular smooth muscle cell proliferation, but also for the prevention of ciclosporin-induced nephrotoxicity. However, there are few clinical reports regarding the interaction between ciclosporin and carvedilol, and the precise mechanism of this interaction has yet to be elucidated. Therefore, we have investigated the effect of carvedilol on the pharmacokinetics of ciclosporin in rats and in the Caco-2 cell line (which expresses P-glycoprotein). Previous reports indicated that blood levels of ciclosporin increased when carvedilol was introduced, and thus the dose of ciclosporin had to be decreased by 20% (Kaijser et al 1997) or 10% (Bader et al 2005). Kaijser et al (1997) speculated that cytochrome P450 enzymes contributed to this interaction. Indeed, ciclosporin is metabolized by CYP3A4, which plays a dominant role in the metabolic elimination of many drugs (Lamba et al 2002). Drugs which are substrates of CYP3A4, including calcium channel blockers, macrolide antibiotics, and antifungal azoles, have been shown to clinically increase the concentrations of ciclosporin in blood (Guan et al 1996; Koselj et al 1994). Carvedilol undergoes extensive metabolism by CYP2D6, CYP3A4, CYP1A2, CYP2E1 and CYP2C9, while CYP2D6 is the rate-limiting enzyme for the overall disposition (Gehr et al 1999; Graff et al 2001). CYP3A4 has a minor influence on the disposition of carvedilol, because the increase in metabolic clearance after treatment with rifampicin, which markedly induced the expression of CYP3A4, contributed only slightly to the increase in total body clearance (Giessmann et al 2004). Therefore, it was presumed that the probability of a drug–drug interaction dependent on CYP3A4 was unlikely. Figure 1B indicates that carvedilol did not interact with ciclosporin during the elimination phase, indicating that the absorption of ciclosporin was increased by carvedilol, as shown in Figure 1A.

The activity of cytochrome P450 affects not only drug elimination, but also the bioavailability of many drugs. Several studies have shown that intestinal CYP3A4 was responsible for the first pass metabolism of orally administered ciclosporin (Gomez et al 1995; Wu et al 1995). However, if carvedilol were to inhibit intestinal CYP3A4, it would also inhibit liver CYP3A4 activity. Therefore, it was quite unlikely that this was the mechanism behind the interaction. On the other hand, Bader et al (2005) suggested that carvedilol influenced ciclosporin levels through its effects on P-glycoprotein in cardiac transplant recipients. We designed an in-vitro study to evaluate the inhibitory effects of carvedilol on ciclosporin transport. Several in-vitro models have been proposed to determine the inhibitory effect or substrate specificity of P-glycoprotein. In this study, we examined the inhibitory effects of carvedilol and verapamil on the intracellular uptake of the P-glycoprotein substrate ciclosporin in Caco-2 cells. The Caco-2 cell line has been used extensively as a model of the intestinal barrier and absorptive properties of the intestinal mucosa. Caco-2 cells express many kinds of transporter proteins such as multidrug resistance-associated proteins, P-glycoprotein, peptide transporters, organic anion transporters, and organic cation transporters (Katsura & Inui 2003). Previous reports indicated that the pharmacokinetics of ciclosporin were related to the expression level of enterocyte P-glycoprotein in renal transplant patients (Lown et al 1997). Additionally, the basolateral to apical transport of ciclosporin is much greater across human MDR1 cDNA-transfected porcine kidney epithelial LLC-PK1 cells than in LLC-PK1 cells (Adachi et al 2001). Therefore, P-glycoprotein is mainly responsible for the cellular extrusion of ciclosporin. Verapamil is also a well established probe that is routinely used to identify compounds that have the potential to inhibit P-glycoprotein.

Carvedilol has been found to be a substrate of P-glycoprotein, which can be considered as another mechanism of drug–drug interaction (Kakumoto et al 2003; Bart et al 2005). Kakumoto et al (2003) indicated that carvedilol inhibited the treatment of anticancer drugs mediated by P-glycoprotein, and that the inhibitory effect was similar to that of verapamil. The results of our study using Caco-2 cells also showed that carvedilol inhibited the transport of ciclosporin mediated by P-glycoprotein, and that this inhibitory effect was comparable with that of verapamil. After long-term oral administration of carvedilol (25 mg/day) to healthy subjects, the peak plasma concentration in extensive metabolizers and poor metabolizers of CYP2D6 was nearly 0.1 and 0.15 μM, respectively (Giessmann et al 2004). This concentration was almost the 20% inhibitory concentration for the transport of ciclosporin obtained in this study. Therefore, there is a possibility of interaction between ciclosporin and carvedilol in the clinical setting.

Kakumoto et al (2003) speculated that the antioxidative effect of carvedilol caused the inhibitory effect on P-glycoprotein-mediated transport. Indeed, it has been reported that high levels of reactive oxygen species, resulting in severe cellular oxidative stress, increased the expression of MDR1 genes (Ziemann et al 1999). However, this was unlikely because in our study only 90-min incubation with carvedilol inhibited the transport of ciclosporin across Caco-2 cells, and a previous study demonstrated a significant increase in mdr1b mRNA expression after two days of treatment with H_2O_2 (Ziemann et al 1999). Further study is needed to clarify the mechanism.

Ciclosporin is also known to inhibit P-glycoprotein-mediated transport (Chiou et al 2002). Carvedilol is not usually trapped in the brain because P-glycoprotein in the blood–brain barrier extrudes carvedilol from the brain. Bart et al (2005) indicated that the amount of carvedilol taken up in the rat brain was increased after pretreatment with ciclosporin. Although we did not monitor the concentration of carvedilol in blood in this study, there is a possibility that carvedilol blood concentration, and also the distribution of carvedilol in the brain, could be increased after co-treatment with ciclosporin. There have been no studies regarding the interaction between carvedilol and ciclosporin in man which focus on carvedilol, but we should be aware of such cases and monitor clinical symptoms closely.

Conclusion

Co-administration with carvedilol increased ciclosporin bioavailability. By using Caco-2 cells, we found that carvedilol caused a concentration-dependent increase in the intracellular accumulation of ciclosporin, and its effect was comparable with that of verapamil. This study has shown that carvedilol

considerably raised the concentration of ciclosporin in blood, and that this interaction was associated with the absorption phase of ciclosporin caused by the inhibition of P-glycoprotein-mediated transport by carvedilol in the intestine.

References

Adachi, Y., Suzuki, H., Sugiyama, Y. (2001) Comparative studies on in vitro methods for evaluating in vivo function of MDR1 P-glycoprotein. *Pharm. Res.* **18**: 1660–1668

Bader, F. M., Hagan, M. E., Crompton, J. A., Gilbert, E. M. (2005) The effect of β-blocker use on cyclosporine level in cardiac transplant recipients. *J. Heart Transplant* **24**: 2144–2147

Bart, J., Dijkers, E. C., Wegman, T. D., de Vries, E. G., van der Graaf, W. T., Groen, H. J., Vaalburg, W., Willemsen, A. T., Hendrikse, N. H. (2005) New positron emission tomography tracer [(11)C]carvedilol reveals P-glycoprotein modulation kinetics. *Br. J. Pharmacol.* **145**: 1045–1051

Chiou, W. L., Wu, T. C., Ma, C., Jeong, H. Y. (2002) Enhanced oral bioavailability of docetaxel by coadministration of cyclosporine: quantitation and role of P-glycoprotein. *J. Clin. Oncol.* **20**: 1951–1952

Gehr, T. W. B., Tenero, D. M., Boyle, D. A., Qian, Y., Sica, D. A., Shusterman, N. H. (1999) The pharmacokinetics of carvedilol and its metabolites after single and multiple dose oral administration in patients with hypertension and renal insufficiency. *Eur. J. Clin. Pharmacol.* **55**: 269–277

Giessmann, T., Modess, C., Hecker, U., Zschiesche, M., Dazert, P., Kunert-Keil, C., Warzok, R., Engel, G., Weitschies, W., Cascorbi, I., Kroemer, H. K., Siegmund, W. (2004) CYP2D6 genotype and induction of intestinal drug transporters by rifampin predict presystemic clearance of carvedilol in healthy subjects. *Clin. Pharmacol. Ther.* **75**: 213–222

Gomez, D. Y., Wacher, V. J., Tomlanovich, S. J., Hebert, M. F., Benet, L. Z. (1995) The effects of ketoconazole on the intestinal metabolism and bioavailability of cyclosporine. *Clin. Pharmacol. Ther.* **58**: 15–19

Graff, D. W., Williamson, K. M., Pieper, J. A., Carson, S. W., Adams, K. F., Cascio, W. E., Patterson, J. H. (2001) Effect of fluoxetine on carvedilol pharmacokinetics, CYP2D6 activity, and autonomic balance in heart failure patients. *J. Clin. Pharmacol.* **41**: 97–106

Guan, D., Wang, R., Lu, J., Wang, M., Xu, C. (1996) Effects of nicardipine on blood cyclosporine levels in renal transplant patients. *Transplant. Proc.* **28**: 1311–1312

Heitmann, M., Davidsen, U., Stokholm, K. H., Rasmussen, K., Burchardt, H., Petersen, E. B. (2002) Renal and cardiac function during alpha1-beta-blockade in congestive heart failure. *Scand. J. Clin. Lab. Invest.* **62**: 97–104

Ishii, Y., Sawada, T., Kubota, K., Fuchinoue, S., Teraoka, S., Shimizu, A. (2005) Injury and progressive loss of peritubular capillaries in the development of chronic allograft nephropathy. *Kidney Int.* **67**: 321–332

Kaijser, M., Johnsson, C., Zezina, L., Backman, U., Dimeny, E., Fellstrom, B. (1997) Elevation of cyclosporin A blood levels during carvedilol treatment in renal transplant patients. *Clin. Transplant.* **11**: 577–581

Kakumoto, M., Sakaeda, T., Takara, K., Nakamura, T., Kita, T., Yagami, T., Kobayashi, H., Okamura, N., Okumura, K. (2003) Effects of carvedilol on MDR1-mediated multidrug resistance: comparison with verapamil. *Cancer Sci.* **94**: 81–86

Katsura, T., Inui, K. (2003) Intestinal absorption of drugs mediated by drug transporters: mechanisms and regulation. *Drug Metab. Pharmacokinet.* **18**: 1–15

Koselj, M., Bren, A., Kandus, A., Kovac, D. (1994) Drug interactions between cyclosporine and rifampicin, erythromycin, and azoles in kidney recipients with opportunistic infections. *Transplant. Proc.* **26**: 2823–2824

Lamba, J. K., Lin, Y. S., Schuetz, E. G., Thummel, K. E. (2002) Genetic contribution to variable human CYP3A-mediated metabolism. *Adv. Drug Deliv. Rev.* **54**: 1271–1294

Lindholm, A. (1991) Factors influencing the pharmacokinetics of cyclosporine in man. *Ther. Drug Monit.* **13**: 465–477

Lown, K. S., Mayo, R. R., Leichtman, A. B., Hsiao, H. L., Turgeon, D. K., Schmiedlin-Ren, P., Brown, M. B., Guo, W., Rossi, S. J., Benet, L. Z., Watkins, P. B. (1997) Role of intestinal P-glycoprotein (mdr1) in interpatient variation in the oral bioavailability of cyclosporine. *Clin. Pharmacol. Ther.* **62**: 248–260

Padi, S. S., Chopra, K. (2002) Salvage of cyclosporine A-induced oxidative stress and renal dysfunction by carvedilol. *Nephron* **92**: 685–692

Park, J., Ha, H., Kim, M. S., Ahn, H. J., Huh, K. H., Kim, Y. S. (2006) Carvedilol inhibits platelet-derived growth factor-induced extracellular matrix synthesis by inhibiting cellular reactive oxygen species and mitogen-activated protein kinase activation. *J. Heart Lung Transplant.* **25**: 683–689

Patel, M. K., Chan, P., Betteridge, L. J., Schachter, M., Sever, P. S. (1995) Inhibition of human vascular smooth muscle cell proliferation by the novel multi-action antihypertensive agent carvedilol. *J. Cardiovasc. Pharmacol.* **25**: 652–657

Ptachcinski, R. J., Venkataramanan, R., Rosenthal, J. T., Burckart, G. J., Taylor, R. J., Hakala, T. R. (1985) Cyclosporine kinetics in renal transplantation. *Clin. Pharmacol. Ther.* **38**: 296–300

Saeki, T., Ueda, K., Tanigawara, Y., Hori, R., Komano, T. (1993) Human P-glycoprotein transports cyclosporin A and FK 506. *J. Biol. Chem.* **268**: 6077–6080

Sambuy, Y., de Angelis, I., Ranaldi, G., Scarino, M. L., Stammati, A., Zucco, F. (2005) The Caco-2 cell line as a model of the intestinal barrier: influence of cell and culture-related factors on Caco-2 cell functional characteristics. *Cell Biol. Toxicol.* **21**: 1–26

Wu, C. Y., Benet, L. Z., Hebert, M. F., Gupta, S. K., Rowland, M., Gomez, D. Y., Wacher, V. J. (1995) Differentiation of absorption and first-pass gut and hepatic metabolism in humans: studies with cyclosporine. *Clin. Pharmacol. Ther.* **58**: 492–497

Zhu, H. J., Wang, J. S., Markowitz, J. S., Donovan, J. L., Gibson, B. B., Gefroh, H. A., Devane, C. L. (2006) Characterization of P-glycoprotein inhibition by major cannabinoids from marijuana. *J. Pharmacol. Exp. Ther.* **317**: 850–857

Ziemann, C., Burkle, A. Kahl, G. F., Hirsch-Ernst, K. I. (1999) Reactive oxygen species participate in mdr1b mRNA and P-glycoprotein overexpression in primary rat hepatocyte cultures. *Carcinogenesis* **20**: 407–414

0022-3565/07/3223-1305–1314$20.00
THE JOURNAL OF PHARMACOLOGY AND EXPERIMENTAL THERAPEUTICS

JPET 322:1305–1314, 2007

Vol. 322, No. 3
124685/3242979
Printed in U.S.A.

Role of *N*-Methyl-D-aspartate Receptors in Antidepressant-Like Effects of σ_1 Receptor Agonist 1-(3,4-Dimethoxyphenethyl)-4-(3-phenylpropyl)piperazine Dihydrochloride (SA-4503) in Olfactory Bulbectomized Rats

Dayong Wang, Yukihiro Noda, Hiroko Tsunekawa, Yuan Zhou, Masayuki Miyazaki, Koji Senzaki, Atsumi Nitta, and Toshitaka Nabeshima

Department of Neuropsychopharmacology and Hospital Pharmacy, Nagoya University Graduate School of Medicine, Nagoya, Japan (D.W., Y.N., H.T., Y.Z., M.M., K.S., A.N., T.N.); Division of Clinical Science in Clinical Pharmacy Practice, Management and Research, Faculty of Pharmacy, Meijo University, Nagoya, Japan (Y.N.); Division of Scientific Affairs, Japanese Society of Pharmacopoeia, Tokyo, Japan (D.W.); Japanese Drug Organization of Appropriate Use and Research, Nagoya, Japan (T.N.); Department of Chemical Pharmacology, Graduate School of Pharmaceutical Sciences, Meijo University, Nagoya, Japan (T.N.); and Research Institute, Fujimoto Pharmaceutical Corporation, Osaka, Japan (H.T.)

Received April 20, 2007; accepted June 6, 2007

ABSTRACT

In the present study, we aimed to investigate the role of *N*-methyl-D-aspartate (NMDA) receptors in the antidepressant-like effects of a σ_1 receptor agonist, 1-(3,4-dimethoxyphenethyl)-4-(3-phenylpropyl)piperazine dihydrochloride (SA-4503), in the olfactory bulbectomized (OB) rat model of depression. A symptomatology-based behavioral investigation was made by reconstructing in OB rats the symptoms of depression, such as psychomotor agitation, loss of interest, and cognitive dysfunction, using a typical antidepressant, desipramine, as a positive control. Repeated treatment with SA-4503 ameliorated the behavioral deficits in OB rats resembling depression symptoms in the open-field test, sexual behavior test, and cued and contextual fear-conditioning test. SA-4503 displayed advantages over desipramine in the sexual behavior test. SA-4503 also reversed the decrease in the protein expression of NMDA receptor subunit (NR)1, but not NR2A or NR2B, in the prefrontal cortex, hippocampus, and amygdala of OB rats. The behavioral and neurochemical effects of SA-4503 were blocked by combined treatment with a specific σ_1 receptor antagonist, *N,N*-dipropyl-2-(4-methoxy-3-(2-phenylethoxy)phenyl)ethylamine monohydrochloride (NE-100). Furthermore, the effects of SA-4503 on the performance of OB rats in the behavioral tests were abrogated by acute treatment with an NMDA receptor antagonist, (−)-5-methyl-10,11-dihydro-5*H*-dibenzo[*a*,*d*]cyclohepten-5,10-imine maleate (MK-801). The present study indicated for the first time that the σ_1 receptor agonist SA-4503 may have effects on depressive symptoms such as agitation, loss of interest, and impaired cognition, which are mediated by NMDA receptors.

This work was supported, in part, by Grants-in-aid for Scientific Research 14370031, 15922139, 16922036, and 17390018 from the Japan Society for the Promotion of Science; by Grant-in-aid for Scientific Research on Priority Areas 16047214 on "Elucidation of glia-neuron network-mediated information processing systems" from the Ministry of Education, Culture, Sports, Science and Technology; by funds from Integrated Molecular Medicine for Neuronal and Neoplastic Disorders (21st Century COE program); by a grant from the Brain Research Center from the 21st Century Frontier Research Program funded by the Ministry of Science and Technology, Republic of Korea; by the Japan Brain Foundation; by the Mitsubishi Pharma Research Foundation; and by the Brain Research Center of the 21st Century Frontier Research Program of the Ministry of Science and Technology, Republic of Korea.

Article, publication date, and citation information can be found at http://jpet.aspetjournals.org.

doi:10.1124/jpet.107.124685.

σ_1 Receptors are particularly concentrated in the limbic structures of the brain, which play important roles in emotion and cognition (Matsuno et al., 1996; Skuza, 2003; Skuza and Wedzony, 2004; Bermack and Debonnel, 2005; Stahl, 2005). Various antidepressants, including tricyclic compounds, selective serotonin reuptake inhibitors, and monoamine oxidase inhibitors, possess affinity and act as agonists for σ_1 receptors (Maurice et al., 2001; Su and Hayashi, 2003). Based on the above-mentioned points, it is hypothesized that σ_1 receptor agonists may act as antidepressants. SA-4503 is

ABBREVIATIONS: SA-4503, 1-(3,4-dimethoxyphenethyl)-4-(3-phenylpropyl)piperazine dihydrochloride; NMDA, *N*-methyl-D-aspartate; NR, *N*-methyl-D-aspartate receptor subunit; PFC, prefrontal cortex; Hip, hippocampus; MK-801, (−)-5-methyl-10,11-dihydro-5*H*-dibenzo[*a*,*d*]cyclohepten-5,10-imine maleate; OB, olfactory bulbectomy/bulbectomized; DES/Des, desipramine; NE-100, *N,N*-dipropyl-2-(4-methoxy-3-(2-phenylethoxy)phenyl)ethylamine monohydrochloride; ANOVA, analysis of variance; Amg, amygdala; 5-HT, 5-hydroxytryptamine (serotonin); Sham, sham-operated; Sal, saline; (+)-SKF-10047, [2*S*-(2α,6α,11*R**)]-1,2,3,4,5,6-hexahydro-6,11-dimethyl-3-(2-propenyl)-2,6-methano-3-benzazocin-8-ol hydrochloride.

a highly selective agonist of σ_1 receptors, with higher binding affinity than a prototypical σ_1 receptor agonist, (+)-SKF-10047 (Matsuno et al., 1996; Guitart et al., 2004). Although it has been reported that SA-4503 facilitates the release of acetylcholine or dopamine and potentiates the function of *N*-methyl-D-aspartate (NMDA) receptors (Bergeron and Debonnel, 1997; Urani et al., 2002) via the activation of σ_1 receptors, the mechanisms underlying the antidepressant-like effects of SA-4503 are not clear.

Although many studies on depression have focused on alterations in the levels of monoamines, recent studies have investigated postsynaptic targets. NMDA receptors play important roles in fundamental functions of neurons. However, the role of NMDA receptors in depression is still not clear. It has been reported that NMDA receptor density or the mRNA expression of NR1 decreases in the prefrontal cortex (PFC) or hippocampus (Hip) of depressive patients (Nowak et al., 1995; Law and Deakin, 2001; Nudmamud-Thanoi and Reynolds, 2004), and long-term use of a specific NMDA receptor antagonist, phencyclidine, induces symptoms of acute anxiety and depression in humans (Liden et al., 1975; De Angelis and Goldstein, 1978). The involvement of NMDA receptors in depression has also been indicated in pharmacological research: repeated treatments with NMDA receptor antagonists, e.g., phencyclidine and MK-801, not only impair performance in the forced swimming test but also prevent the behavioral and neurochemical effects of antidepressant treatments (De Montis et al., 1993; Meloni et al., 1993; Petrie et al., 2000; Javitt, 2004).

The olfactory bulbectomized (OB) rat has been proposed as a model of depression, exhibiting several essential symptomatic isomorphisms, such as psychomotor agitation, loss of interest, and impaired learning and memory (Holmes, 2003). The olfactory bulbs have extensive neural connections with the structures of the limbic system and other parts of the brain, and they influence many emotional aspects of behavioral and other brain output functions (Jesberger and Richardson, 1985). Bilateral olfactory bulbectomy in rodents produces neuroanatomical deficits analogous to the cortical/allocortical degeneration in depressive patients that is, in general, not dependent on particular structures (Holmes, 2003).

The present symptomotology-based study was conducted to investigate the antidepressant-like effects of the σ_1 receptor agonist SA-4503 and the role of NMDA receptors in the effects, using OB rats as a model of depression, since OB rats have dysfunctional glutamatergic systems (Kelly et al., 1997). In the present study, a tricyclic antidepressant, desipramine, was selected as a positive control to compare the σ_1 receptor- and non-σ_1 receptor-mediated effects, based on the fact that desipramine is a typical antidepressant and its affinity for σ_1 receptors is the weakest of the antidepressants presently in clinical use and several hundred times weaker than that of SA-4503 (Matsuno et al., 1996; Narita et al., 1996).

Materials and Methods

Animals. Five-week-old male Sprague-Dawley rats (170–200 g), were purchased from Japan SLC (Shizuoka, Japan). All rats were housed in our Animal Experimental Center, at a room temperature of 25 ± 1°C and a relative humidity of 40 to 60%. The rooms were illuminated from 9:00 AM to 9:00 PM. All experiments were performed following the Guidelines for Animal Experiments of Nagoya University, which conformed to the international guidelines set out in the *Guide for the Care and Use of Laboratory Animals* (Institute of Laboratory Animal Resources, 1996).

Medicines and Reagents. SA-4503 was provided by M's Science Corporation (Kobe, Japan). Desipramine hydrochloride (DES), NE-100, and (+)-MK-801 were purchased from Sigma-Aldrich (St. Louis, MO). Goat polyclonal anti-NR1, NR2A, and NR2B IgG recognizing protein bands of approximately 103, 180, and 200 kDa and horseradish peroxidase-conjugated donkey anti-goat IgG were purchased from Santa Cruz Biotechnology, Inc. (Santa Cruz, CA). The anti-NR1 antibody has an epitope mapping at the C terminus of $NR1_{011}$ (938 amino acids in rat brain; approximately 103 kDa), which is also known as ζ1, NR1a, or NMDAR1-1a, and is the predominant form of the eight splices of NR1 in adult rat brain (Laurie and Seeburg, 1994; Zukin and Bennett, 1995).

Surgical Procedure. The rats were anesthetized with 60 mg/kg pentobarbital sodium, and then they were fixed on a stereotactic apparatus (Narishige, Tokyo, Japan). A midline sagittal incision was made to expose the skull overlaying the olfactory bulbs. A hole 4 mm in diameter was made through the skull 6 mm anterior to the bregma. The olfactory bulbs were cut with a microknife, and they were aspirated out using a pipette tip connected with a water suction pump, with care being taken not to damage the frontal cortex. The cavity for the olfactory bulbs was filled with hemostatic sponge. The hole in the skull was covered with a piece of gelatin gauze, and the skin was sutured. Sham-operated rats were treated in a similar way, except that the olfactory bulbs were not removed. The success of the operation was anatomically confirmed after all of the behavioral tests, and the data from the maloperated rats were excluded from the subsequent analysis.

Schedule of Drug Administration and Behavioral Tests. The schedule of drug administration and behavioral tests is shown in Fig. 1. Saline, desipramine, SA-4503, and/or NE-100 was s.c. administered daily 2 weeks after the surgery for 16 days. MK-801 was s.c. injected 30 min before testing or training trials.

Open-Field Test. The present protocol was adapted from those of Kameyama et al. (1980) and Kelly and Leonard (1994). The open field apparatus, painted gray, consisted of a square arena (60 × 60 cm) divided into 15-cm squares by black lines. The wall of the arena was 30 cm in height. A 60-watt light bulb was positioned at the center 90 cm above the base of the arena.

On the 29th day after the operation, ambulation and rearing

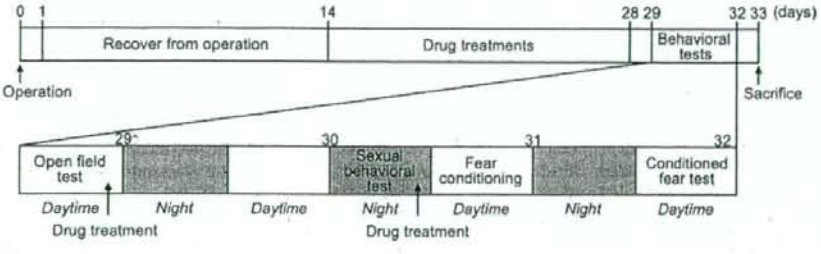

Fig. 1. Schedule of operation, drug treatment, and behavioral tests.

frequencies were recorded in the first 3 min immediately after each rat entered the arena. After each test, the apparatus was sprayed with 70% alcohol, and it was wiped thoroughly to eliminate residual odor.

Sexual Behavior Test. The present protocol was adapted from that of Breigeiron et al. (2002). The apparatus for the sexual behavior test consisted of a transparent Plexiglas box [45 (length) × 27 (width) × 39.5 (height) cm] with a black plastic base, illuminated with a red lamp. On the 30th day after the operation, the sexual behavior of individual male OB rats was observed for 30 min between 10:00 PM and 3:00 AM. A male rat was first placed in the Plexiglas box to habituate to the environment for 3 min. Then, a sexually receptive normal female rat was introduced that had been s.c. administered 0.14 mg of estradiol 72 and 48 h before the test and 0.7 mg of progesterone 4 h before the test. The following parameters of sexual behavior were recorded: starting latency of genital probing and thrusting, count of genital probing and thrusting, and the percentage of the rats that probed the female genitals or showed thrusting behavior. After each test, the apparatus was sprayed with 70% alcohol, and it was wiped thoroughly to eliminate residual odor.

Cued and Contextual Fear-Conditioning Test. The present protocol was adapted from those of Mamiya et al. (2003) and Phillips and LeDoux (1992). The apparatus consisted of a transparent Plexiglas box [45 (length) × 27 (width) × 39.5 (height) cm; the neutral box] with a black plastic base and a Perspex box [32 (length) × 26 (width) × 48 (height) cm; the conditioning box] with a steel grid floor connected to an electric shock generator (Neuroscience-Idea Co., Ltd., Osaka, Japan) and enclosed in an opaque compartment. The neutral box was illuminated with a red lamp, and the conditioning box was illuminated with a fluorescent lamp (6 watt).

For measuring basal levels of the freezing response (preconditioning phase), on the 31st day after the operation, rats were individually placed in the neutral box for 1 min and then in the conditioning box for 2 min. For conditioning (conditioning phase), a 60-s tone (75 dB) was presented as a conditioned stimulus. Just before the end of the tone, a 0.5-mA electric foot-shock lasting for 0.5 s was delivered as an unconditioned stimulus. The tone and the electric foot-shock ceased together. It should be noted that a 0.5-mA electric current lasting for 0.5 s in only one training session was not strong enough to form a stable conditioned response in all of the rats; hence, a difference in the ability to learn and memorize could be observed.

Cued and contextual tests were carried out 24 h after the conditioning. For the cued test, the freezing response was measured in the neutral box for 1 min in the presence of the tone. For the contextual test, rats were placed in the conditioning box, and the freezing response was measured for 2 min in the absence of the tone and foot shock. The freezing response was defined as follows: all four paws of the rat remaining still and the animal stooped down with fear. After each test, the apparatus was sprayed with 70% alcohol and wiped thoroughly to eliminate residual odor.

Western Blot Analysis. After all of the behavioral tests, the rats were sacrificed by decapitation. The dorsal PFC, the CA1-CA3 and dentate gyrus of the Hip, and the posteromedial and posterolateral cortical amygdaloid nuclei of the Amg were rapidly dissected out according to the atlas of the brain of the rat (Paxinos and Watson, 1998). Brain samples were frozen and stored at −80°C until used. The brain samples were homogenized in 150 μl of ice-cold lysis buffer [50 mM Tris-HCl, 150 mM NaCl, 1 mM sodium orthovanadate, 10 mM EDTA, 10 mM NaF, 0.1% SDS, 1% Igepal CA-630 (Sigma-Aldrich), 1% sodium deoxycholate, 10 μg/ml aprotinin, 10 μg/ml leupeptin, 10 μg/ml pepstatin, and 0.5 mM DL-dithiothreitol] using an ultrasonic processor (Astrason, Farmingdale, NY). After homogenization, the lysates were kept in an ice bath for 20 min, and then they were centrifuged at 13,000 rpm for 20 min at 4°C. The protein concentration of supernatants was determined by Lowry's method (Lowry et al., 1951). Samples of equal protein concentration were made by mixing the supernatants with lysis buffer, diluting 1:1 with sample-loading buffer (100 mM Tris, 200 mM DL-dithiothreitol, 4% SDS, 0.2% bromphenol blue, and 20% glycerol, pH 6.8), and heating at 95°C for 5 min. Different samples with a protein concentration of 30 μg/10 μl were electrophoresed by SDS-polyacrylamide gel electrophoresis (PAGE) (6–15% step-gradient resolving gel, an upper 6% gel used for the separation of NMDA receptor subunits, and a lower 15% gel for the separation of β-actin), transferred to polyvinylidene difluoride membranes, and incubated in block solution. The membranes were then incubated overnight with anti-NR1, NR2A, or NR2B antibody (1:1000) at 4°C. After wash, the membranes were incubated with horseradish peroxidase-conjugated secondary antibodies at room temperature for 1 h, and then they were washed thoroughly. The bands on membranes were then visualized, and the light absorbance was analyzed using an ATTO Densitograph Software Library Lane Analyzer (Atto Co., Tokyo, Japan).

Statistical Analysis. Statistical differences were evaluated with a one-way analysis of variance (ANOVA), except for the evaluation of the time-dependent change in body weight, for which a two-way ANOVA was used. The modified Tukey's test was applied after ANOVA tests for multiple comparisons. The difference in the percentage of rats that showed genital-probing and thrusting behavior among the groups in the sexual behavioral test was evaluated with the χ^2 test. The criterion for a statistically significant difference was $p < 0.05$.

Results

Antidepressant-Like Effects of SA-4503 in OB Rats

Open-Field Test. The open-field test is the behavioral test most commonly used to evaluate the antidepressant-like

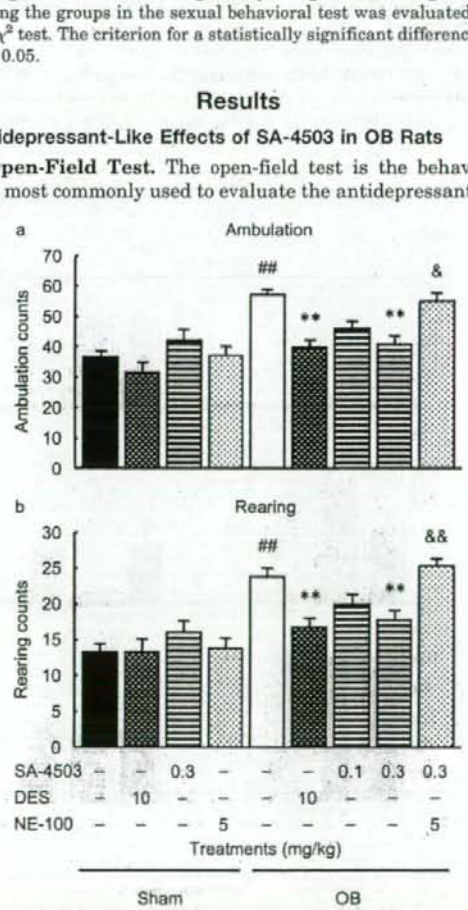

Fig. 2. Effects of repeated treatment with SA-4503 on performance of the open-field test in OB rats. a, ambulation counts in the first 3 min of the test. b, rearing counts in the first 3 min of the test. Results are expressed as means ± S.E., $n = 16–18$. ##, $p < 0.01$, versus saline-treated sham-operated rats; **, $p < 0.01$, versus saline-treated OB rats; &, $p < 0.05$ and &&, $p < 0.01$, versus SA-4503 (0.3 mg/kg)-treated OB rats. Sham, sham-operated rats.

effects of medicines using the OB rat model. As shown in Fig. 2, a and b, saline-treated OB rats exhibited significantly increased counts of ambulation [$F_{(8,141)} = 10.088$; $p < 0.01$] and rearing [$F_{(8,141)} = 8.168$; $p < 0.01$] in the first 3 min after being put into the open-field arena. The exploratory hyperactivity in OB rats was reversed by the repeated treatments both with 10 mg/kg desipramine and 0.3 mg/kg SA-4503. The effects of SA-4503 were abolished by the combined treatment with 5 mg/kg NE-100. Desipramine at 10 mg/kg, SA-4503 at 0.3 mg/kg, and NE-100 at 5 mg/kg did not significantly affect behavior in sham-operated rats. Interestingly, the counts of ambulation and rearing decreased in OB rats compared with sham-operated rats from 6 to 9 min after the animals were put into the open-field arena. These data are not shown because these counts are not commonly adopted as experimental indices in the open-field test using OB rats.

Sexual Behavior Test. The loss of interest shown in depressive patients is a core symptom of depression as depicted in the Diagnostic and Statistical Manual, Version IV (Seidman and Roose, 2001). As an alternative measure, we examined the effect of the σ_1 receptor agonist SA-4503 on the sexual dysfunction. As shown in Fig. 3, the starting latency of genital probing [$F_{(8,141)} = 29.466$; $p < 0.01$] and thrusting [$F_{(8,141)} = 6.343$; $p < 0.01$] was increased in saline-treated OB rats (Fig. 3, a and d), whereas the number of genital-probing [$F_{(8,141)} = 13.300$; $p < 0.01$] and thrusting events [$F_{(8,141)} = 4.178$; $p < 0.01$] (Fig. 3, b and e) and the percentage of the rats that showed genital-probing and thrusting behavior (Fig. 3, c and f) were decreased, compared with values for sham rats. These results showed sexual deficits in OB rats.

Treatment with 0.3 mg/kg SA-4503 reduced the deficits of genital-probing and thrusting behavior in OB rats without affecting the behavior in sham-operated rats (Fig. 3). The effects of SA-4503 on sexual behavior were blocked by NE-100 (Fig. 3). Repeated treatment with desipramine at the dose of 10 mg/kg ameliorated the loss of genital-probing behavior (Fig. 3, a–c), without affecting thrusting behavior (Fig. 3, d–f).

Cued and Contextual Fear-Conditioning Test. Major depressive patients exhibit significant cognitive dysfunction, to which minor depression is not related (Murphy et al., 1998; Airaksinen et al., 2004; Stordal et al., 2004). In the preconditioning phase of the test, all the rats showed a similar freezing time either in the neutral box or in the conditioning box (data not shown). Twenty-four hours after conditioning, OB rats exhibited a significantly shortened freezing time in both the cued [$F_{(8,116)} = 8.783$; $p < 0.01$] and contextual

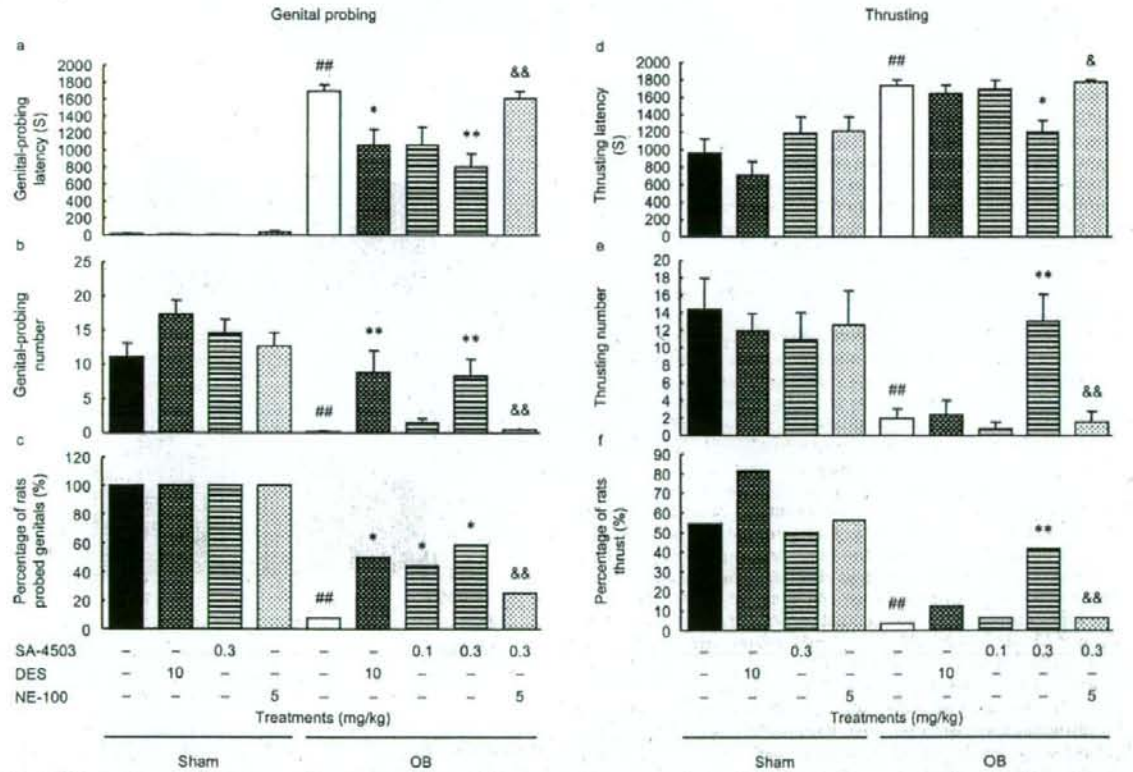

Fig. 3. Effects of repeated treatment with SA-4503 on sexual behavior in OB rats. a, genital-probing starting latency. b, genital-probing number. c, percentage of rats probing the female genital. d, thrusting latency. e, thrusting number. f, percentage of rats that showed penis-thrusting behavior. Results are expressed as means ± S.E. or percentages, $n = 16–18$. ##, $p < 0.01$, versus saline-treated sham-operated rats; *, $p < 0.05$ and **, $p < 0.01$, versus saline-treated OB rats; &, $p < 0.05$ and &&, $p < 0.01$, versus 0.3 mg/kg SA-4503-treated OB rats. Statistical differences of percentages among the groups were analyzed with the χ^2 test.

[$F_{(8,116)} = 10.440$; $p < 0.01$] tests compared with sham-operated rats (Fig. 4, a and b).

In both the cued and contextual tests, the cognitive deficits in OB rats were reversed by repeated treatment with 10 mg/kg desipramine and SA-4503 (0.3 mg/kg in cued test and 0.1 and 0.3 mg/kg in contextual test; Fig. 4, a and b). The effects of SA-4503 were blocked by NE-100 at the dose of 5 mg/kg (Fig. 4, a and b). In preliminary experiments, no change in the response threshold was found in saline- and drug-treated OB rats: the minimal current intensities required to elicit flinching/running, jumping, or vocalization in saline- and drug-treated OB rats were the same as those in sham-operated control rats (data not shown).

Involvement of NMDA Receptors in the Effects of SA-4503

Because 0.1 and 0.3 mg/kg SA-4503 significantly improved the behavioral abnormalities in OB rats in a dose-dependent manner, the dose of 0.3 mg/kg was used in all subsequent experiments.

Effects of SA-4503 on Protein Expression of NRs. As shown in Fig. 5, the protein expression of NR1 decreased in the PFC [$F_{(4,50)} = 19.055$; $p < 0.01$], Hip [$F_{(4,50)} = 4.274$; $p < 0.01$], and Amg [$F_{(4,50)} = 19.399$; $p < 0.01$] of saline-treated OB rats compared with sham-operated control rats. The loss of NR1 was ameliorated by the treatments with 10 mg/kg desipramine and 0.3 mg/kg SA-4503. The improving effects of

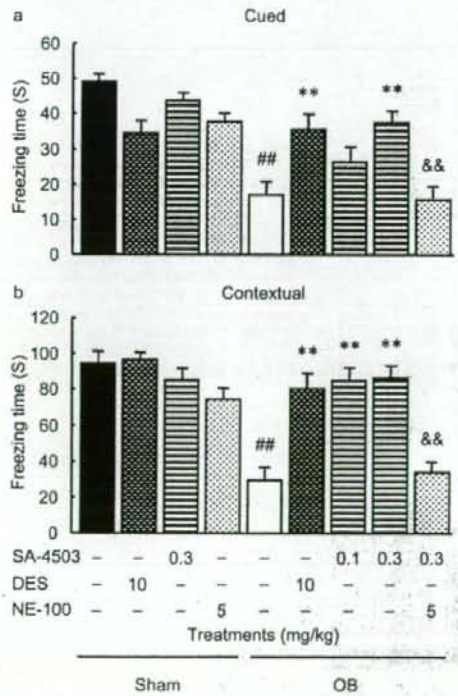

Fig. 4. Effects of repeated treatment with SA-4503 on performance of cued and contextual conditioning test in OB rats. a, freezing time in the cued test. b, freezing time in the contextual test. Results are expressed as means ± S.E., $n = 12$–14. ##, $p < 0.01$, versus saline-treated sham-operated rats; **, $p < 0.01$, versus saline-treated OB rats; &&, $p < 0.01$, versus 0.3 mg/kg SA-4503-treated OB rats.

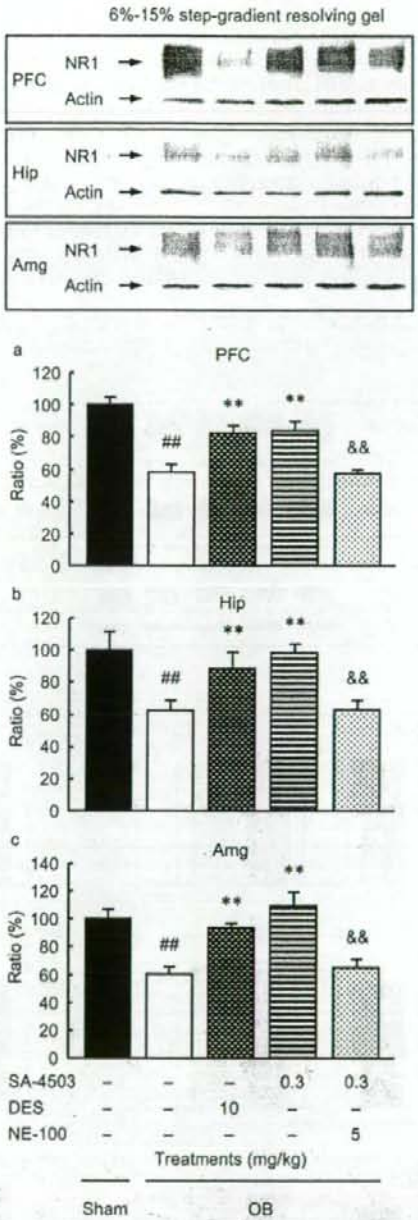

Fig. 5. Effects of repeated treatment with SA-4503 on protein expression of NR1 in the prefrontal cortex, hippocampus, and amygdala of OB rats. a, in the PFC. b, in the Hip. c, in the Amg. Results are expressed as means ± S.E., $n = 11$. ##, $p < 0.01$, versus saline-treated sham-operated rats; **, $p < 0.01$, versus saline-treated OB rats; &&, $p < 0.01$, versus 0.3 mg/kg SA-4503-treated OB rats. Proteins were separated by SDS-PAGE on 6 to 15% step-gradient resolving gels.

SA-4503 on the protein expression of NR1 in these regions in OB rats were blocked by 5 mg/kg NE-100. There was no significant difference in the protein expression of NR2A or NR2B in these regions between sham-operated and OB con-

trol rats (Fig. 6). These results are consistent with previous publications on the density and function of NMDA receptors in the brain of OB rats, and they fit well with reports that the expression of NR1 decreases in the brain of depressive patients (Kelly et al., 1997; Law and Deakin, 2001; Robichaud et al., 2001; Nudmamud-Thanoi and Reynolds, 2004).

Open-Field Test. As shown in Fig. 7, the treatment with MK-801 at 0.03 mg/kg blocked the effect of 0.3 mg/kg SA-4503 on the exploratory hyperactivity in OB rats. The treatment with MK-801 at 0.03 mg/kg tended to increase the counts of ambulation [$F_{(4,85)} = 11.143$; $p < 0.01$] and rearing [$F_{(4,85)} = 11.230$; $p < 0.01$] in the sham-operated rats.

Sexual Behavior Test. The effects of 0.3 mg/kg SA-4503 on the latency of genital probing [$F_{(4,75)} = 38.257$; $p < 0.01$] and thrusting [$F_{(4,75)} = 4.797$; $p < 0.01$] (Fig. 8, a and d), the number of genital-probing [$F_{(4,75)} = 6.784$; $p < 0.01$] and thrusting events [$F_{(4,75)} = 3.850$; $p < 0.01$] (Fig. 8, b and e), and the percentage of animals that probed the female genitals and showed thrusting behavior (Fig. 8, c and f) were blocked by the treatment with MK-801 at 0.03 mg/kg, a dose that did not significantly affect sexual behavior in the sham-operated rats (Fig. 8).

Cued and Contextual Fear-Conditioning Test. The treatment with MK-801 at 0.03 mg/kg blocked the effects of 0.3 mg/kg SA-4503 in both the cued [$F_{(4,49)} = 15.305$; $p < 0.01$] and contextual [$F_{(4,49)} = 13.493$; $p < 0.01$] tests (Fig. 9, a and b). At the dose of 0.03 mg/kg, the treatment with MK-801 significantly impaired the performance of sham-operated rats (Fig. 9, a and b).

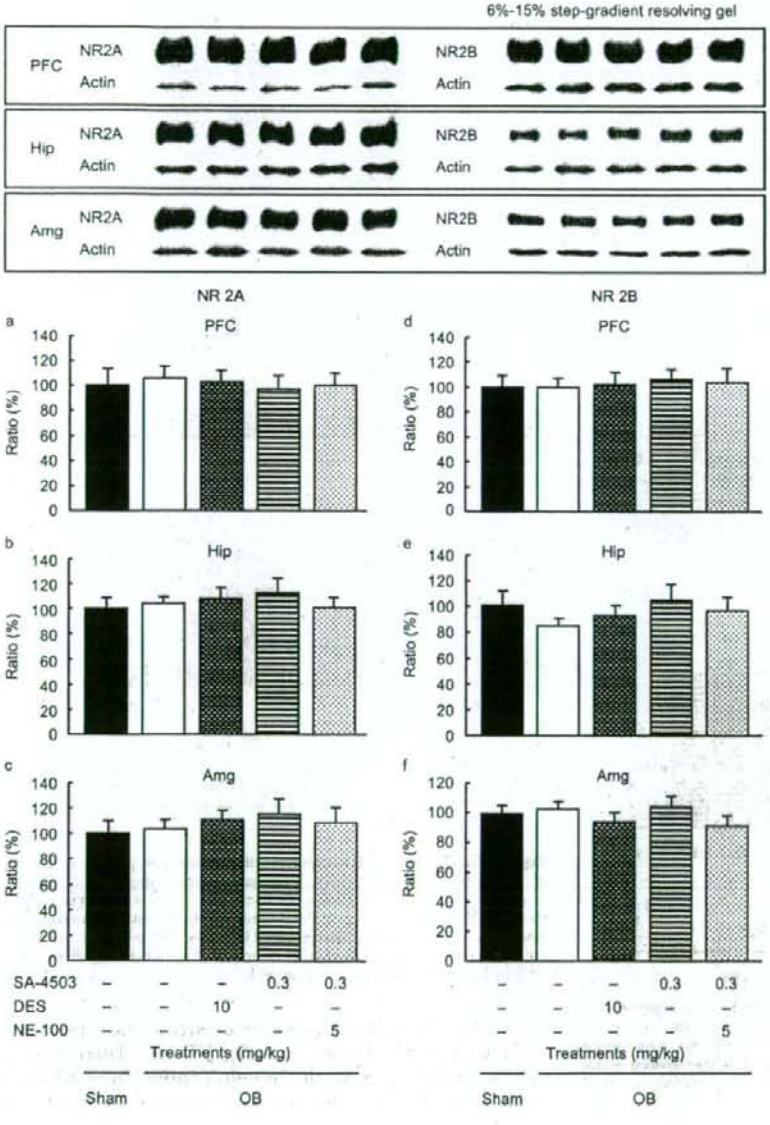

Fig. 6. Effects of repeated treatment with SA-4503 on protein expression of NR2A and NR2B in the prefrontal cortex, hippocampus, and amygdala of OB rats. a, protein expression of NR2A in the PFC. b, protein expression of NR 2A in the Hip. c, protein expression of NR2A in the Amg. d, protein expression of NR2B in the PFC. e, protein expression of NR2B in the Hip. f, protein expression of NR2B in the Amg. Results are expressed as means ± S.E., $n = 10$. Proteins were separated by SDS-PAGE on 6 to 15% step-gradient resolving gels.

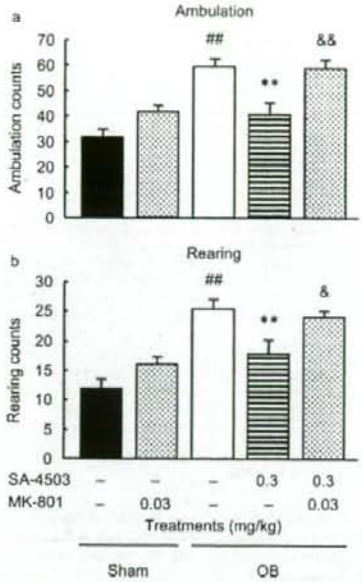

Fig. 7. Effects of SA-4503 on performance of the open-field test in OB rats were abolished by MK-801. a, ambulation counts. b, rearing counts. Results are expressed as means ± S.E., $n = 18$. ##, $p < 0.01$, versus saline-treated sham-operated rats; **, $p < 0.01$, versus saline-treated OB rats; &, $p < 0.05$ and &&, $p < 0.01$, versus 0.3 mg/kg SA-4503-treated OB rats.

Changes in Body Weight of Sham-Operated and OB Rats Treated with Saline and Medicines

Olfactory bulbectomy induced the decrease of body weight in rats. Treating OB rats with SA-4503 at the dose of 0.3 mg/kg partially reversed the decrease of the body weight. In contrast to the treatment with SA-4503, repeated treatment with desipramine at the dose of 10 mg/kg decreased the body weight of OB rats [$F_{\text{group (3,2897)}} = 222.742$; $p < 0.01$; and $F_{\text{time (28,2897)}} = 485.303$; $p < 0.01$] (Fig. 10).

Discussion

The OB rat is considered to be one of the best animal models of depression in terms of construct validity (Jesberger and Richardson, 1988; Lumia et al., 1992; Kelly et al., 1997; van der Stelt et al., 2005). Chronic deprivation of olfaction, the primary sensory mode in rats, constitutes a stress of high intensity, and the behavioral deficits induced by OB are primarily the result of alterations in neuronal functions, which is supported by the phenomenon that the behavioral deficits can be reversed by antidepressant treatments although the olfactory bulbs are nonexistent (van Riezen et al., 1977; Jesberger and Richardson, 1988; Mar et al., 2000; O'Neil and Moore, 2003). The depression symptom-resembling deficits in OB rats can be normalized by chronic, not acute, antidepressant treatments (Jesberger and Richardson, 1985; Kelly et al., 1997). In previous preliminary study, treating OB rats with SA-4503 for 1 week did not significantly ameliorate the behavioral deficits, which were ameliorated after treating for 2 weeks in the present study.

Desipramine, a conventional tricyclic antidepressant that inhibits the reuptake of norepinephrine and 5-HT, was used as a positive control. The binding affinity of desipramine ($K_i \approx 1987$ nM) for σ_1 receptors is approximately 450 times weaker than that of SA-4503 ($K_i \approx 4.4$ nM; $IC_{50} \approx 17.4$ nM) (Narita et al., 1996; Shiba et al., 2006), and it takes effects mainly by inhibiting the reuptake of norepinephrine ($IC_{50} \approx 8.3$ nM) or 5-HT ($IC_{50} \approx 17.5$ nM) at the present dose (Pi et al., 1986; Hyttel, 1993). We also treated rats with imipramine at the dose of 20 mg/kg; however, the subcutaneous or intraperitoneal treatment induced severe inflammation in the rats. Therefore, imipramine-treated rats were not fit for behavioral analyses in the emotional study. Selective serotonin reuptake inhibitors were not preferred as control agents, given that they increase the risk of suicide-related behavior, especially in adolescents (Fegert and Herpertz-Dahlmann, 2005).

The open-field test is most commonly used for screening antidepressants using OB rat model. Within the initial 3 min in a stressful environment, OB rats show hyperlocomotion, which resembles the psychomotor agitation in depression, the extreme of which is a suicidal impulse (Lumia et al., 1992; Holmes, 2003). Based on the predictive value of the open-field test, it was suggested that SA-4503 may have antidepressant-like effects, which is further supported by the results of the sexual behavioral and the fear-conditioning tests.

Patients with major depression exhibit symptoms of sexual and cognitive dysfunction, which have been proven to be unrelated to minor depression and dysthesia (Murphy et al., 1998; Seidman and Roose, 2001; Airaksinen et al., 2004; Stordal et al., 2004). Alternatively, the sexual dysfunction in OB rats resembles the loss of interest that is a core symptom of depression. The result with the sexual dysfunction in OB rats is consistent with previous publications (Mathew et al., 1980; Mathew and Weinman, 1982). Compared with SA-4503, desipramine had relatively weak effects on sexual behavior in OB rats. It improved genital-probing behavior, rather than thrusting behavior, indicating a combination of positive effects and latent side effects of desipramine and that SA-4503 may have therapeutic advantages over it.

Major depression is associated with cognitive impairments (Murphy et al., 1998; Airaksinen et al., 2004; Stordal et al., 2004). Studies have reported spared functions in depressed patients in tests tapping implicit memory (Hertel and Hardin, 1990; Danion et al., 1995), explicit memory (Bazin et al., 1994), and attention (Landro et al., 2001). In the present study, an impairment of associative learning and long-term memory involving the Hip and Amg was observed in OB rats in the fear-conditioning test, which fits well with some clinical observations demonstrating explicit memory deficits in depressive patients (Vythilingam et al., 2004; Kieseppa et al., 2005). The performance of OB rats in both the cued and contextual tests was improved by desipramine and SA-4503. These results indicated that SA-4503 may ameliorate the cognitive symptoms of depression.

NMDA receptors play fundamental roles in the mammalian nervous system. They also have neurotrophic effects, and NR1 null animals cannot survive (Augustine et al., 1987; Malenka, 1994; Mohn et al., 1999; Balazs, 2006). Dysfunctional central nervous system glutamatergic pathways may be one of pathophysiological factors in depression (Nudmamud-Thanoi and Reynolds, 2004), and magnetic resonance imaging revealed a reduced level of glutamate in the

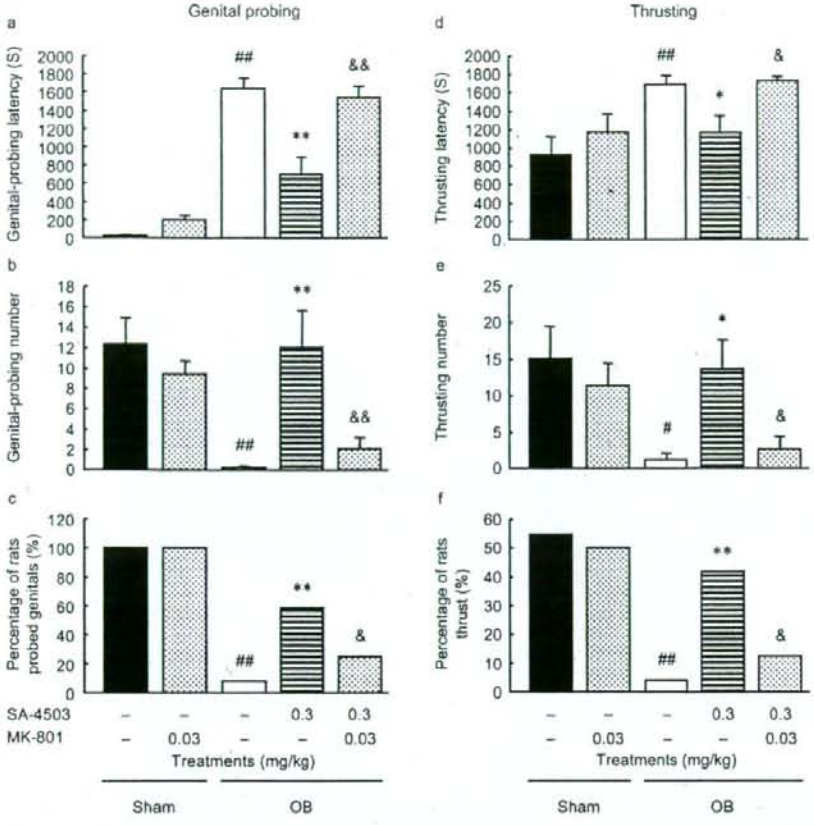

Fig. 8. Effects of SA-4503 on sexual behavior in OB rats were abolished by MK-801. a, genital-probing starting latency. b, genital-probing number. c, percentage of rats that probed the female genital. d, thrusting latency. e, thrusting number. f, percentage of rats that showed penis-thrusting behavior. Results are expressed as means ± S.E. or percentages, $n = 16$. #, $p < 0.05$ and ##, $p < 0.01$, versus saline-treated sham-operated rats; *, $p < 0.05$ and **, $p < 0.01$, versus saline-treated OB rats; &, $p < 0.05$ and &&, $p < 0.01$, versus 0.3 mg/kg SA-4503-treated OB rats. Statistical differences of percentage among the groups were analyzed with the χ^2 test.

PFC, which returned to normal following treatments with antidepressants (Bermack and Debonnel, 2005). Law and Deakin (2001) have reported that the expression of NR1 decreases in the hippocampus of depressive patients. The NMDA receptor density and the immunoreactivity of NR1 also decrease in other brain structures in depressive patients (Nudmamud-Thanoi and Reynolds, 2004). Furthermore, NMDA receptor density is decreased in the frontal cortex of suicide victims of depression, and the adaptation of the density to repeated antidepressant treatments has been ruled out (Nowak et al., 1995).

NR1 is indispensable for diverse NMDA receptors, and it is functional in a homomeric form; however, NR2 subunits require NR1 to form functional complexes (Zukin and Bennett, 1995). NR1 is distributed ubiquitously in the brain. In contrast, NR2 subunits are region-specifically distributed. NR2A is distributed widely, with relatively high levels in the cerebral cortex, the Hip, and cerebellar granule cells. NR2B is expressed selectively in the forebrain, with high levels in the cerebral cortex, hippocampal formation, septum, caudate-putamen, olfactory bulbs, and thalamus. The NR2C subunit is found predominantly in the cerebellum, whereas weak expression is detected in the olfactory bulbs and the thalamus. NR2D is expressed at much lower levels than the other subunits, and it is found in the thalamus, brainstem, and olfactory bulbs (Liu and Zhang, 2000). The deficit in the protein expression of NR1 underlies the decreased density and function of NMDA receptors in the OB rat brain (Kelly et al., 1997; Robichaud et al., 2001). Hei et al. (2006) have reported that NR1 expression was increased by activation of NMDA receptors that coexist with and are potentiated by σ_1 receptors (Bergeron and Debonnel, 1997; Urani et al., 2002), which indicates a mechanism for the effect of SA-4503 on protein expression of NR1.

The affinities of SA-4503 for α_1, D_2, 5-HT_{1A}, 5-HT_2, H_1, M_1, and M_2 receptors are at least 100 times weaker than that for the σ_1 receptors (Matsuno et al., 1996). In the present study, all the effects of SA-4503 were blocked by the σ_1 receptor antagonist NE-100 at a low dose, which confirmed that the effects of SA-4503 are basically mediated by σ_1 receptors.

The behavioral effects of SA-4503 were blocked by an NMDA receptor antagonist, MK-801. This result is at least partially supported by the report that the mice expressing 5–10% NR1 exhibit sexual dysfunction (Mohn et al., 1999). The decrease in the protein expression of NR1 is just one facet of neurodegeneration in the OB rat brain, and NMDA receptors play a crucial role in the emotional effects of SA-4503, because the compensatory phenomena evident in sham-operated rats were not observed in SA-4503-treated OB rats.

Besides having a role in emotion, NMDA receptors are involved in the cognitive effects of SA-4503 in the fear-conditioning test, which is supported by the report that the Hip-regional knockout of NR1 inhibits the ability of animals